Aconicatisulfonines A and B, Analgesic Zwitterionic C_{20}-Diterpenoid Alkaloids with a Rearranged Atisane Skeleton from *Aconitum carmichaelii*

Yuzhuo Wu,[†] Shuai Shao,[†] Qinglan Guo, Chengbo Xu, Huan Xia, Tiantai Zhang,[*] and Jiangong Shi[*]

State Key Laboratory of Bioactive Substance and Function of Natural Medicines, Institute of Materia Medica, Chinese Academy of Medical Sciences and Peking Union Medical College, Beijing 100050, People's Republic of China

Contents of Supporting Information

Experimental Section

General Experimental Procedures. The optical rotation was measured on a P-2000 polarimeter (JASCO, Tokyo, Japan). The UV spectra was recorded on a V-650 spectrometer (JASCO). The CD spectrum was measured on a JASCO J-815 CD spectrometer (JASCO). The IR spectrum was recorded on a Nicolet 5700 FT-IR Microscope spectrometer (FT-IR Microscope Transmission) (Thermo Electron Corporation, Madison, WI, USA). 1D- and 2D-NMR spectra were obtained at 600 MHz for ^{1}H and 150 MHz for ^{13}C, respectively, on a SYS 600 MHz (Varian Associates Inc., Palo Alto, CA, USA) or Bruker AVANCE III HD 600 MHz spectrometer with (δ_H = 4.800) and CD_3OD or CH_3OH (δ_C = 49.50) as references for ^{1}H and ^{13}C, respectively. HRESIMS data were obtained on an Agilent 6520 Accurate-Mass Q-TOF LCMS spectrometer (Agilent Technologies, Ltd., Santa Clara, CA, USA). Column chromatography (CC) was performed with macroporous adsorbent resin (HPD-110, Cangzhou Bon Absorber Technology Co. Ltd, Cangzhou, China), MCI gel (CHP 20P, 75–150 μm, Mitsubishi Chemical Corporation, Tokyo, Japan), reversed phase C-18 silica gel (Ultrapure Silica Dels, Silicycle, Canada), HW-40F (Toyopearl, Tosoh, Japan), and Sephadex LH-20 (Pharmacia Biotech AB, Uppsala, Sweden). HPLC separation was performed on a system consisting of an Agilent ChemStation for LC system, an Agilent 1200 pump, and an Agilent 1100 single-wavelength absorbance detector (Agilent Technologies, Ltd) or a Smartline RI detector (Knauer, Berlin, Germany) detector, using a Capcell Pak ADME column (250 × 10 mm i.d.) (Shiseido Co., Ltd, Japan). TLC was conducted on precoated silica gel GF_{254} plates. Spots were visualized under UV light (254 or 356 nm) or by spraying with 5% H_2SO_4 in 95% EtOH followed by heating or with a Dragendorff's reagent. Unless otherwise noted, all chemicals were obtained from commercially available sources and were used without further purification.

Plant Material. The lateral root of *Aconitum carmichaelii* Debx was collected in June 2009 from the culture field in Jiangyou, Sichuan Province, People's Republic of China. Plant identity was verified by Dr. Yan Ren (Chengdu University of TCM, Sichuan 610075, China). A voucher specimen (no. ID-S-2383) was deposited at the herbarium of the Department of Medicinal Plants, Institute of Materia Medica, Chinese Academy of Medical Sciences & Peking Union Medical College, Beijing 100050, China.

Extraction and Isolation. The air-dried lateral roots of *A. carmichaelii* (50 kg) were powdered and extracted with H_2O (3 × 150 L × 6 h) at 40 °C. The H_2O extract was concentrated to 120 L under reduced pressure, subjected to chromatography over a macroporous adsorbent resin (HPD-110, 19 kg) column (20 × 200 cm), and eluted successively with H_2O (50 L), 30% EtOH (120 L), 50% EtOH (120 L), and 95% EtOH (100 L) to afford the corresponding fractions A–D. After removal of the solvent, fraction C (3.5 kg) was chromatographed over MCI gel (CHP 20P) with successive elution using H_2O (10 L), 30% EtOH (30 L), 50% EtOH (20 L), and 95% EtOH (10 L) to give fraction C1–C4. Fraction C1 (750 g) was chromatographed over reversed phase C-18 silica gel, eluting with a gradient increasing CH_3OH (0→50%) in H_2O (80 L), then with 100% CH_3OH (10 L), to yield corresponding subfractions C1-1 – C1-12 based on TLC analysis. Subfration C1-4 (75 g) was fractionated by CC over Sephadex LH-20 (H_2O) to afford C1-4-1 – C1-4-4, of which C1-4-3 (26 g) was rechromatographed over reversed phase C-18 silica gel (10→15% CH_3OH in H_2O) to yield C1-4-3-1 – C1-4-3-10. Separation of C1-4-3-8 (20 g) by CC over reversed phase C-18 silica gel with an isocratic elution of 6% CH_3OH in H_2O obtained C1-4-3-8-1 – C1-4-3-8-7, of which C1-4-3-8-6 (12 g) was further chromatographed over HW-40F, eluting with 6% CH_3OH in H_2O, to give C1-4-3-8-6-1 – C1-4-3-8-6-21. Reseparation of C1-4-C-8-6-7 (2 g) by CC over HW-40F eluting with CH_2Cl_2-CH_3OH (1:1) afforded C1-4-3-8-6-7-1 – C1-4-3-8-6-7-8. Isolation of C1-4-3-8-6-7-7 (52 mg) by HPLC using the ADME column (14% CH_3CN in H_2O, containing 0.5% TFA, flow rate 2.0 mL/min) afforded **1** (3.4 mg, t_R = 14 min) and **2** (1.1 mg, t_R = 21 min).

Aconicatisulfonine A (**1**): Colorless prisms (CH_3OH-H_2O, 5:1), m.p. > 300 °C; $[\alpha]^{20}_D$ –34.5 (*c* 0.33, H_2O); UV (H_2O) λ_{max} (log ε) 232.8 (3.84) nm; CD (H_2O) λ_{max} ($\Delta\varepsilon$) 215.5 (+2.87), 244.5 (+3.65) nm; IR ν_{max} 3507, 3445, 2958, 2930, 2863, 2585, 2530, 1674, 1614, 1466, 1448, 1427, 1395, 1374, 1312, 1273, 1228, 1186, 1110, 1086, 1046,1023,1007, 984, 938, 868, 850, 823, 791, 775, 704, 661, 636, 604, 579, 539, 503, 486 cm^{-1}; ^{1}H NMR (D_2O, 600 MHz) data, see Table 1; ^{13}C NMR (D_2O, 150 MHz) data, see Table 1; (+)-HRESIMS *m/z* 422.1991 $[M + H]^+$ (calcd. for $C_{22}H_{32}NO_5S$, 422.1996); (–)-HRESIMS *m/z* 420.1844 $[M - H]^-$ (calcd. for $C_{22}H_{30}NO_5S$, 420.1850).

Aconicatisulfonine B (**2**): White amorphous powder; $[\alpha]^{20}_D$ –56.3 (*c* 0.08, H_2O); UV (H_2O) λ_{max} (log ε) 203.0 (3.03), 275.0 (sh, 1.76) nm; CD (H_2O) λ_{max} ($\Delta\varepsilon$) 222 (+4.08) nm; IR ν_{max} 3382, 2942, 2877, 1678, 1425, 1202, 1139,1034, 879, 867, 838, 802, 766, 723, 671, 626, 561 cm^{-1}; ^{1}H NMR (D_2O, 600 MHz) data, see Table 1; ^{13}C NMR (D_2O, 150 MHz) data, see Table 1; (+)-HRESIMS *m/z* 424.2152 $[M + H]^+$ (calcd. for $C_{22}H_{34}NO_5S$, 424.2152); (–)-HRESIMS *m/z* 422.2009 $[M - H]^-$ (calcd. for $C_{22}H_{32}NO_5S$, 422.2007).

Conformational Analysis and Calculations of the ECD and UV Spectra of 1 and 2.[S1] Conformational analysis and quantum computations were performed using Gaussian 16 program package.[S2] Conductor-like polarizable continuum model (CPCM) was adopted to consider solvent effects using the dielectric constant of H_2O (ε = 78.36).

Conformational searches of **1** and **2** showed 20 and 11 lowest energy conformers with relative energy within 10 kcal/mol, respectively. After re-optimized using HF at 6-31g level, the conformers with boltzmann distributions larger than 1% and without virtual frequency (Table S1 and Figure S3 for **1** and Table S2 and Figure S5 for **2**) were calculated using the TDDFT methodology at the B3LYP/6-311g (d, p) level for their energies, oscillator strengths, rotational strengths. The ECD and UV spectra were simulated by the Gaussian function (σ = 0.24 eV). The final spectra of **1** (Figure S4) and **2** (Figure S6) were accomplished by averaging of relative conformational Gibbs free energy (G) combined with UV correction, respectively. For the enantiomers, the ECD spectra were depicted by inverting the final spectra of **1** and **2**.

X-ray Crystallography of 1. monoclinic, space group $P2_1$ (no. 4), a = 8.1008 (3) Å, b = 16.2916 (9) Å, c = 8.2497 (3) Å, α = 90°, β = 98.027 (4)°, γ = 90°, V = 1078.08 (8) Å^3, Z = 2, μ (Cu Kα) = 1.720, 6942 reflections measured, 4055 unique (R_{int} = 0.0240), wR_2 = 0.0788 (all data), goodness of fit = 1.097, Flack parameter –0.001 (6).

The data were collected on a Gemini E diffractometer with Cu Kα radiation by using the ω scan technique with 2θ values from 10.83° to 142.24°. The crystal was kept at 108 (6) K during data collection. Using Olex2,[S3] the structure was solved with the

SIR2004[S4] structure solution program using Direct Methods and refined with the SHELXL[S5] refinement package using CGLS minimisation. The absolute configuration was determined on the basis of the Flack parameter −0.001 (6). Crystallographic data for the structure of **1** have been deposited with the Cambridge Crystallographic Data Centre as supplementary publication (CCDC 1936199). Copies of these data can be obtained free of charge via www.ccdc.cam.ac.uk/conts/retrieving.html (or from the Cambridge Crystallographic Data Centre, 12 Union Road, Cambridge CB21EZ, UK; fax: (+44) 1223-336-033; or deposit@ccdc.cam.ac.uk).

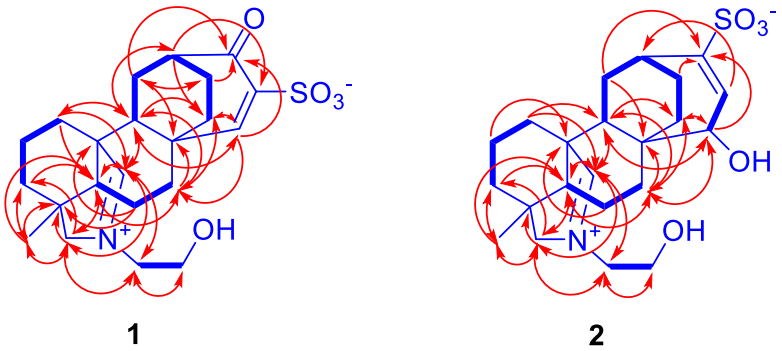

1 **2**

Figure S1. The detailed ^{1}H-^{1}H COSY (thick lines) and HMBC correlations (red arrows, from ^{1}H to ^{13}C) of **1** and **2**

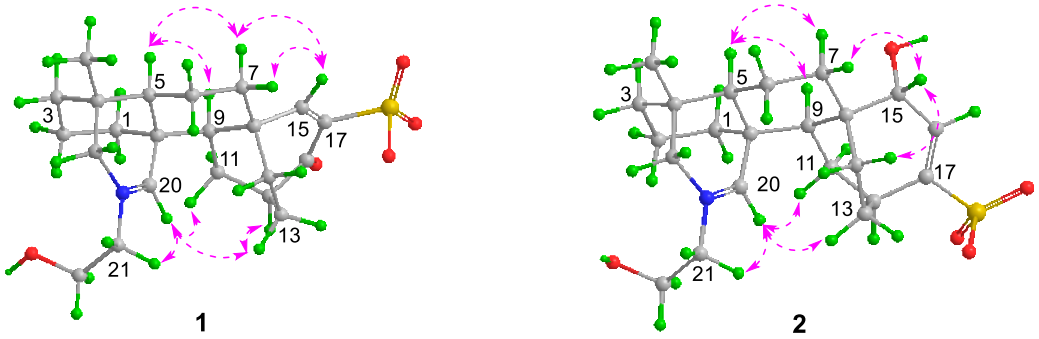

1 **2**

Figure S2. Main NOE enhancements (pink dash lines with double arrows) of **1** and **2**.

Table S1. Relative Energy and Boltzmann Distribution for Conformers of 1.

	MMFF94		HF/6-31g		B3LYP/6-311G(d,p)	
Conf.	rel. E kcal/mol	Boltzmann distribution	E Hartree	Boltzmann distribution	E Hartree	Boltzmann distribution
1C1	30.30710	72.32%	-1676.4992207	2.71%	-1686.3378550	2.95%
1C2	30.88020	27.47%	-1676.4992174	2.70%	-1686.3391013	11.07%
1C3	34.41550	0.07%	-1676.4934851	0.01%		
1C4	34.62680	0.05%	-1676.5021457	60.22%	-1686.3397641	22.36%
1C5	34.99680	0.03%	-1676.4999796	6.06%	-1686.3394755	16.46%
1C6	35.01580	0.03%	-1676.4992208	2.71%	-1686.3379091	3.13%
1C7	35.40400	0.01%	-1676.4931286	0.00%		
1C8	35.63530	0.01%	-1676.4964963	0.15%		
1C9	35.99410	0.00%	-1676.4964963	0.15%		
1C10	36.16200	0.00%	-1676.4966958	0.19%		
1C11	36.95600	0.00%	-1676.4999796	6.06%	-1686.3394645	16.27%
1C12	37.19440	0.00%	-1676.4992174	2.70%	-1686.3391024	11.09%
1C13	37.59430	0.00%	-1676.4989590	2.06%	-1686.3348372	0.12%
1C14	37.91230	0.00%	-1676.4999628	5.96%	-1686.3353737	0.21%
1C15	38.15510	0.00%	-1676.4966959	0.19%		
1C16	38.25150	0.00%	-1676.4999796	6.06%	-1686.3394608	16.21%
1C17	38.28480	0.00%	-1676.4916111	0.00%		
1C18	38.57820	0.00%	-1676.4989590	2.06%	-1686.3391013	0.12%
1C19	39.02140	0.00%	-1676.4934852	0.01%		
1C20	39.39480	0.00%	-1676.4911997	0.00%		

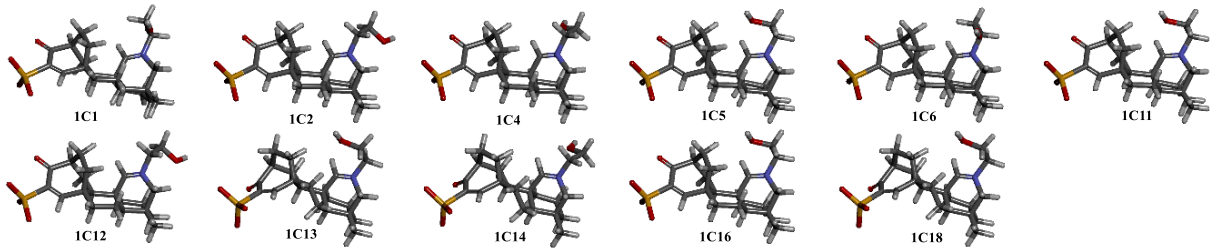

Figure S3. The key 3D conformers of **1** obtained by re-optimization at HF/6-31g.

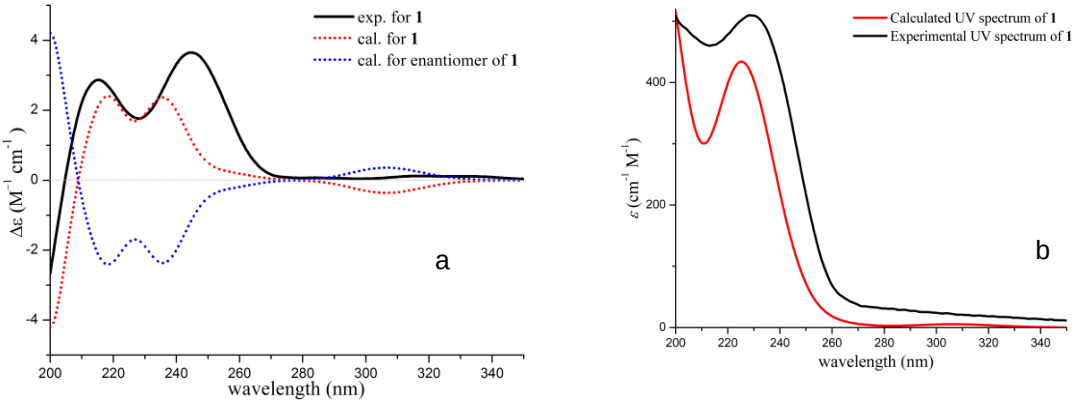

Figure S4. (a) The overlaid experimental CD spectrum of **1** (black line) and the calculated ECD spectra of **1** (red line) and its enantiomer (blue line). (b) The overlaid experimental (black line) and calculated (red line) UV spectra of **1**.

Table S2. Relative Energy and Boltzmann Distribution for Conformers of 2.

	MMFF94		HF/6-31g		B3LYP/6-311G(d,p)	
Conf..	rel. E kcal/mol	Boltzmann distribution	E Hartree	Boltzmann distribution	E Hartree	Boltzmann distribution
2C1	59.7236	49.93%	-1677.684743	10.62%	-1687.5405604	8.18%
2C2	60.0349	29.52%	-1677.684719	10.36%	-1687.5415228	22.68%
2C3	60.424	15.30%	-1677.68649	67.64%	-1687.5420016	37.68%
2C4	61.0618	5.21%	-1677.684144	5.63%	-1687.5418272	31.32%
2C5	64.8121	0.01%	-1677.683318	2.35%	-1687.5361615	0.08%
2C6	64.8121	0.01%	-1677.683318	2.35%	-1687.5361615	0.08%
2C7	64.9759	0.01%	-1677.682299	0.80%		
2C8	65.0816	0.01%	-1677.680126	0.08%		
2C9	65.1236	0.01%	-1677.680756	0.16%		
2C10	65.8203	0.00%	-1677.678824	0.02%		
2C11	66.3174	0.00%	-1677.678441	0.01%		

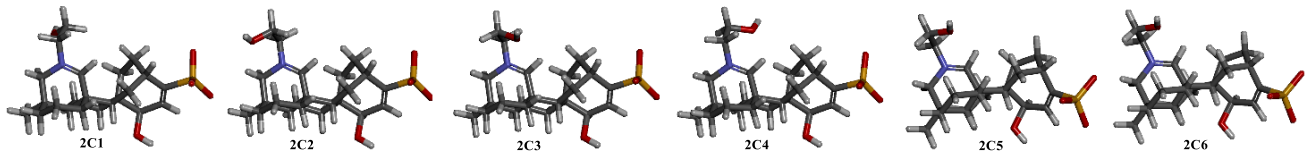

Figure S5. The key 3D conformers of **2** obtained by re-optimization at HF/6-31g.

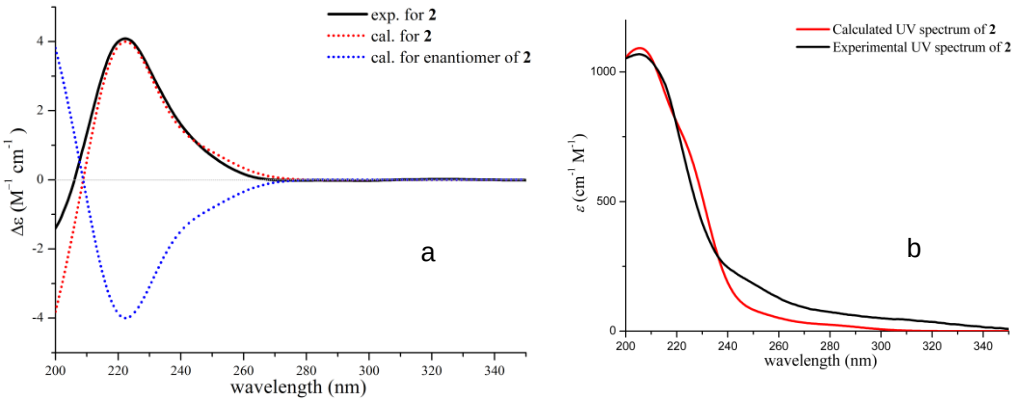

Figure S6. (a) The overlaid experimental CD spectrum of **2** (black line) and the calculated ECD spectra of **2** (red line) and its enantiomer (blue line). (b) The overlaid experimental (black line) and calculated (red line) UV spectra of **2**.

Acetic Acid-Induced Writhing Test of Compounds 1 and 2. An acetic acid-induced writhing method was adopted for the evaluation of analgesic activity of compounds **1** and **2**. Briefly, ICR female mice were randomly divided into groups (eight mice per group), and pre-treated intraperitoneally with normal saline (the vehicle group), morphine (0.3 mg/kg, the positive control group), and compounds **1** or **2** (1.0 mg/kg, 0.3 mg/kg, and 0.1 mg/kg, the three test groups), respectively. 30 min later, mice were treated by intraperitoneal injection of 1.0% v/v acetic acid solution (0.1 ml/kg). The number of writhing was recorded for 15 min. The analgesic effects of the test compound and positive control were respectively expressed by decreasing the number of writhes compared to normal saline. Percent inhibition was calculated using formula as below:

Percent inhibition = [(Wm-Wt)/Wm] × 100%

Where *Wm* is the number of writhing of the vehicle group, and *Wt* is the number of writhing of test group or positive group.

The results showed that compounds **1** and **2** significantly reduced the number of writhing induced by acetic acid in a dose-dependent manner (Table S3 and Figure S7).

Table S3. Experimental Data for Evaluation of the Analgesic effect of Compounds 1 and 2.

Groups	Reagents	Number	Dose (mg/kg)	Number of writhing	Percent inhibition (%)
Vehicle group	Normal saline	8	-	36.5±2.4	-
Positive group	morphine	8	0.3	12.1±2.1***	66.82
Test group	Compound **1**	8	0.1	28.0±3.3	23.29
Test group	Compound **1**	8	0.3	20.8±3.1**	43.15
Test group	Compound **1**	8	1.0	18.1±3.1***	50.34
Test group	Compound **2**	8	0.1	19.5±5.5**	46.57
Test group	Compound **2**	8	0.3	12.9±2.1***	64.73
Test group	Compound **2**	8	1.0	8.9±5.3***	75.68

Note: Data are expressed as mean ± SEM, $^{**}p < 0.01$, $^{***}p < 0.001$ compared to vehicle group.

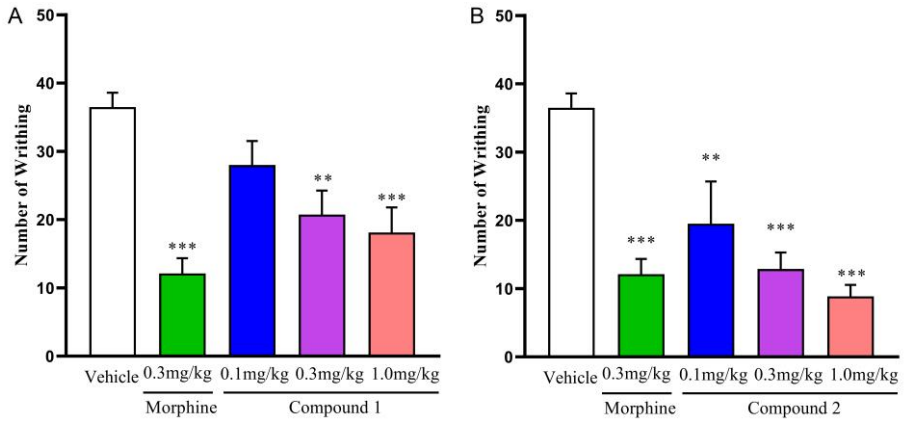

Figure S7. Analgesic effects of compound**s** against acetic acid-induced writhing of mice. (A) The analgestic effects of compound **1**; (B) The analgestic effects of compound **2**. The data were expressed as mean ± SEM, $^{**}p < 0.01$, $^{***}p < 0.001$ compared to vehicle group.

Scheme S1. The Plausible Biosynthetic Pathways of 1 and 2 via the precursor atisine (3′)

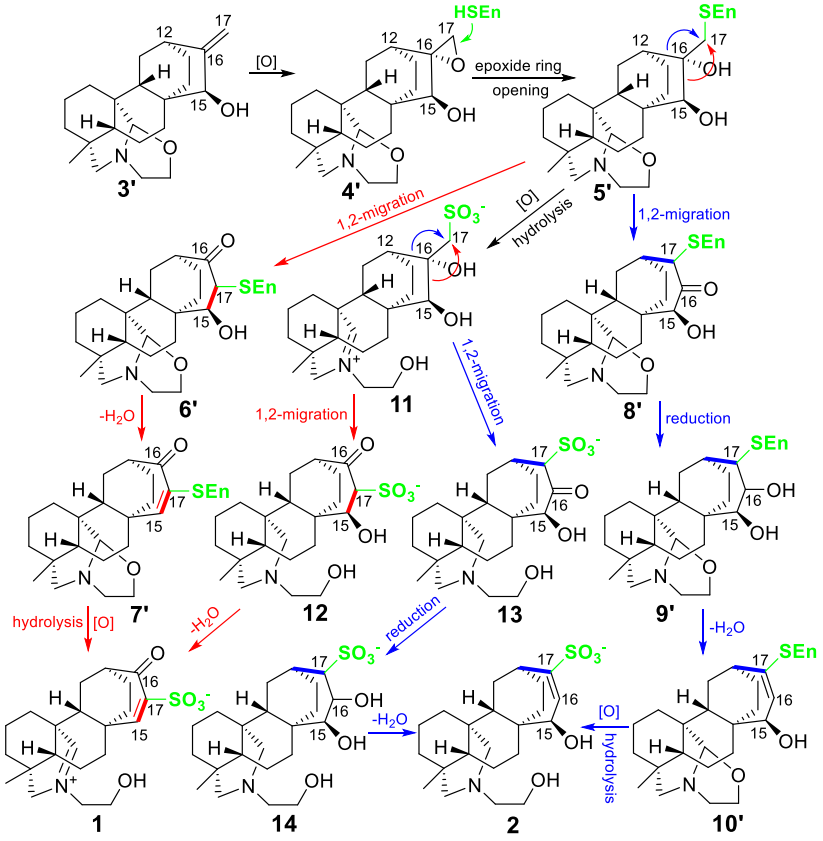

References

(S1) (a) Li, X.-C.; Ferreira, D.; Ding, Y.-Q. *Curr. Org. Chem.* **2010**, *14*, 1678–1697. (b) Chianese, G.; Fattorusso, E.; Aiyelaagbe, O. O.; Luciano, P.; Schroder, H. C.; Müller, W. E. G.; Taglialatela-Scafati, O. *Org. Lett.* **2011**, *13*, 316–319.

(S2) Frisch, M. J.; Trucks, G. W.; Schlegel, H. B.; Scuseria, G. E.; Robb, M. A.; Cheeseman, J. R.; Scalmani, G.; Barone, V.; Petersson, G. A.; Nakatsuji, H.; Li, X.; Caricato, M.; Marenich, A. V.; Bloino, J.; Janesko, B. G.; Gomperts, R.; Mennucci, B.; Hratchian, H. P.; Ortiz, J. V.; Izmaylov, A. F.; Sonnemberg, J. L.; Williams-Young, D.; Ding, F.; Lipparini, F.; Egidi, F.; Goings, J.; Peng, B.; Petrone, A.; Henderson, T.; Ranasinghe, D.; Zakrzewski, V. G.; Gao, J.; Rega, N.; Zheng, G.; Liang, W.; Hada, M.; Ehara, M.; Toyota, K.; Fukuda, R.; Hasegawa, J.; Ishida, M.; Nakajima, T.; Honda, Y.; Kitao, O.; Nakai, H.; Vreven, T.; Throssell, K.; Montgomery, J. A., Jr.; Peralta, J. E.; Ogliaro, F.; Bearpark, M.; Heyd, J. J.; Brothers, E.; Kudin, K. N.; Staroverov, V. N.; Keith, T. A.; Kobayashi, R.; Normand, J.; Raghavachari, K.; Rendell, A.; Burant, J. C.; Iyengar, S. S.; Tomasi, J.; Cossi, M.; Millam, J. M.; Klene, M.; Adamo, C.; Cammi, R.; Ochterski, J. W.; Martin, R. L.; Morokuma, K.; Farkas, O.; Foresman, J. B.; Fox, D. J. *Gaussian 16, Revision A.03*; Gaussian, Inc.: Wallingford, CT, 2016.

(S3) Dolomanov, O. V.; Bourhis, L. J.; Gildea, R. J.; Howard, J. A. K.; Puschmann, H. *J. Appl. Cryst.* **2009**, *42*, 339–341.

(S4) Burla, M. C.; Caliandro, R.; Camalli, M.; Carrozzini, B.; Cascarano, G. L.; De Caro, L.; Giacovazzo, C.; Polidori, G.; Siliqi, D.; Spagna, R. *J. Appl. Cryst.* **2007**, *40*, 609–613.

(S5) Sheldrick, G. M. *Acta Cryst.* **2008**, *A64*, 112–122.

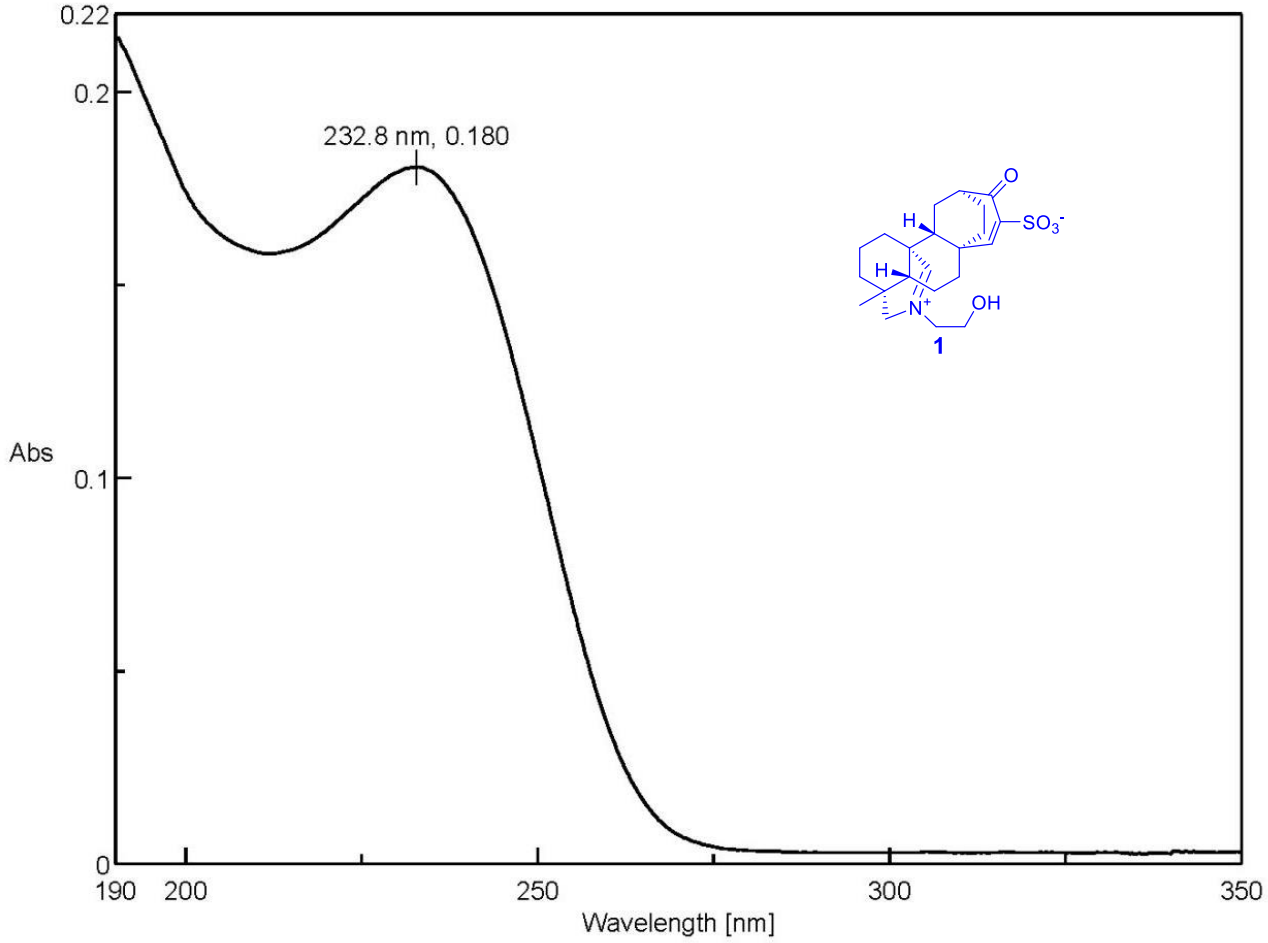

w-46

[Comment]
Sample Name w-46
Comment
User
Division UV
Company
[Measurement Information]
Instrument Name V-650
Model Name V-650
Serial No. A034461150

Accessory PSC-718
Accessory S/N A001761114
Position 2
Cell Length 10 mm
Temperature 20.02 C
Control Sonsor Holder
Monitor Sensor Holder
Start Mode Start immediately

Photometric Mode Abs
Measurement range 600 - 190 nm
Data pitch 0.2 nm
Band width(UV/Vis) 2.0 nm
Response Medium
Scanning speed 200 nm/min
Source Change 340 nm
Light Source D2/WI
Filter Exchange Step
Correction Baseline

[Data Information]
Creation Date 2019-4-17 14:56

Data array type Linear data array
Horizontal Wavelength [nm]
Vertical Abs
Start 600 nm
End 190 nm
Data pitch 0.2 nm
Data points 2051

Figure S8. The UV spectrum of compound **1** in H_2O.

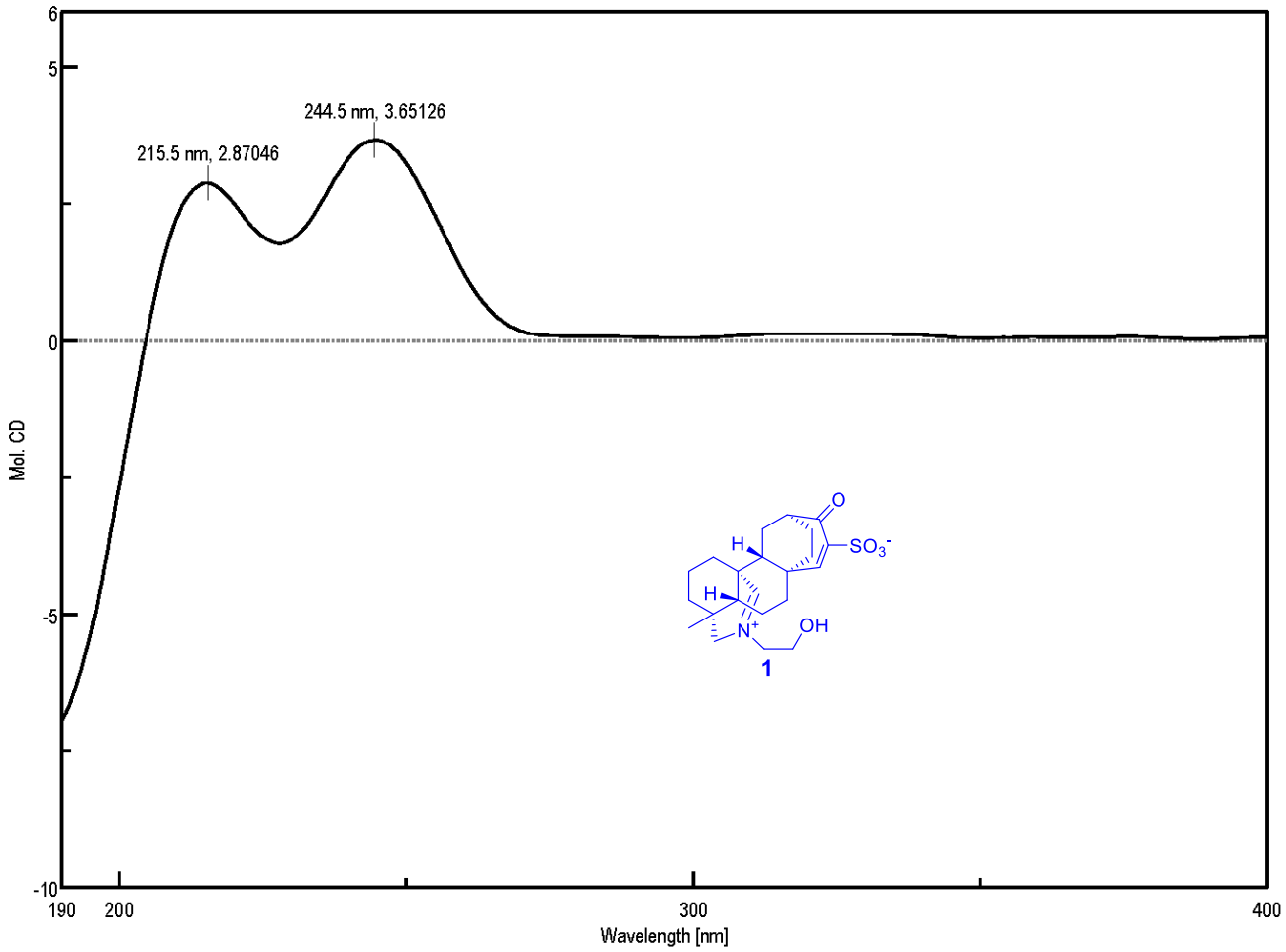

W-46-1-s-m.jws

[Measurement Information]	
Instrument Name	J-815
Model Name	J-815
Serial No.	A024461168
Accessory	Standard
Accessory S/N	A024461168
Cell Length	1 mm
Measurement date	2019/4/17 9:06
Photometric Mode	CD, HT, Abs
Measure Range	400 - 190 nm
Data pitch	0.5 nm
Sensitivity	Standard
D.I.T.	1 sec
Bandwidth	1.00 nm
Start Mode	Immediately
Scanning Speed	100 nm/min
Baseline Correction	Baseline
Shutter Control	Auto
CD Detector	PMT
PMT Voltage	Auto
Accumulations	2
Solvent	H2O
Concentration	0.33 (w/v)%

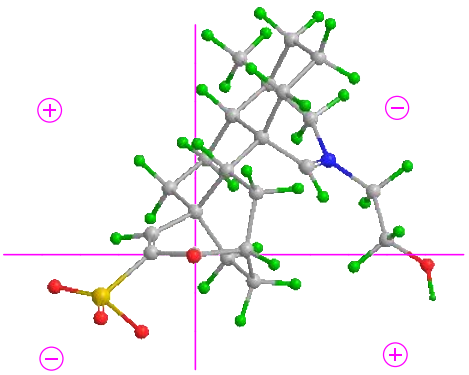

Figure S9. The CD spectrum of compound **1** in H_2O and the octant rule to predict the absolute configuration of compound **1**.

Thermo Qexactive Focus Report

compound NO. : W-46

Method : LCMS(compound)-low

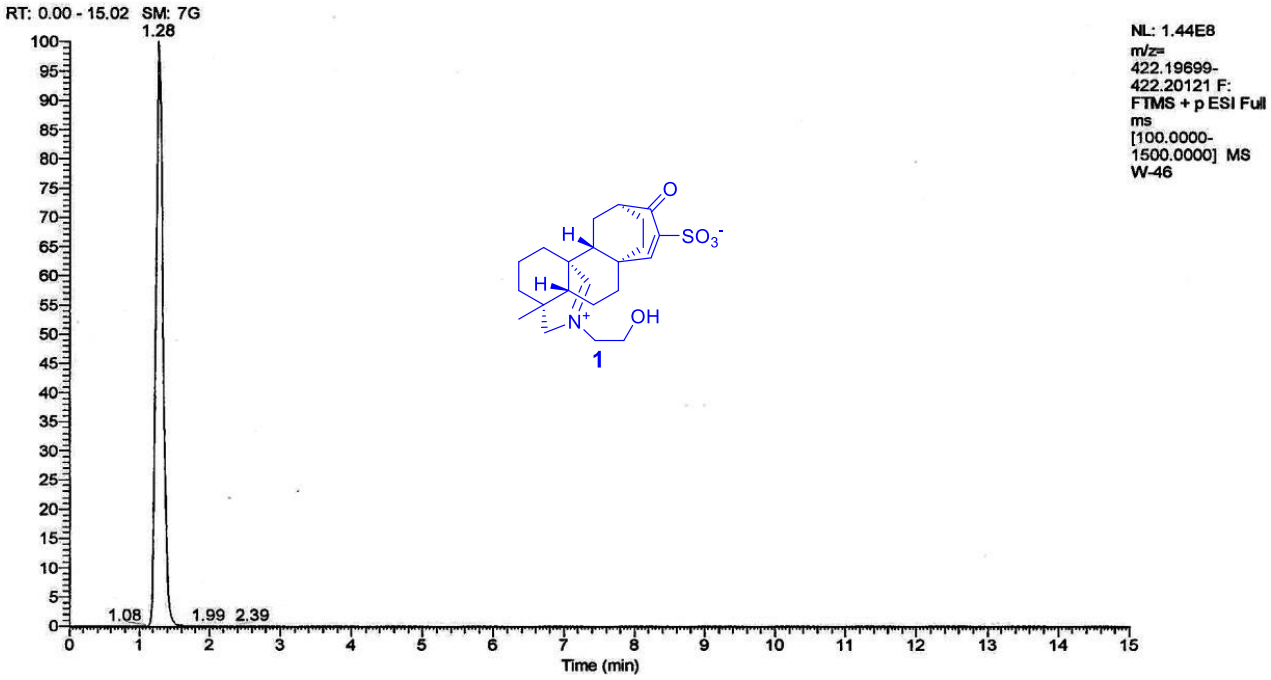

1

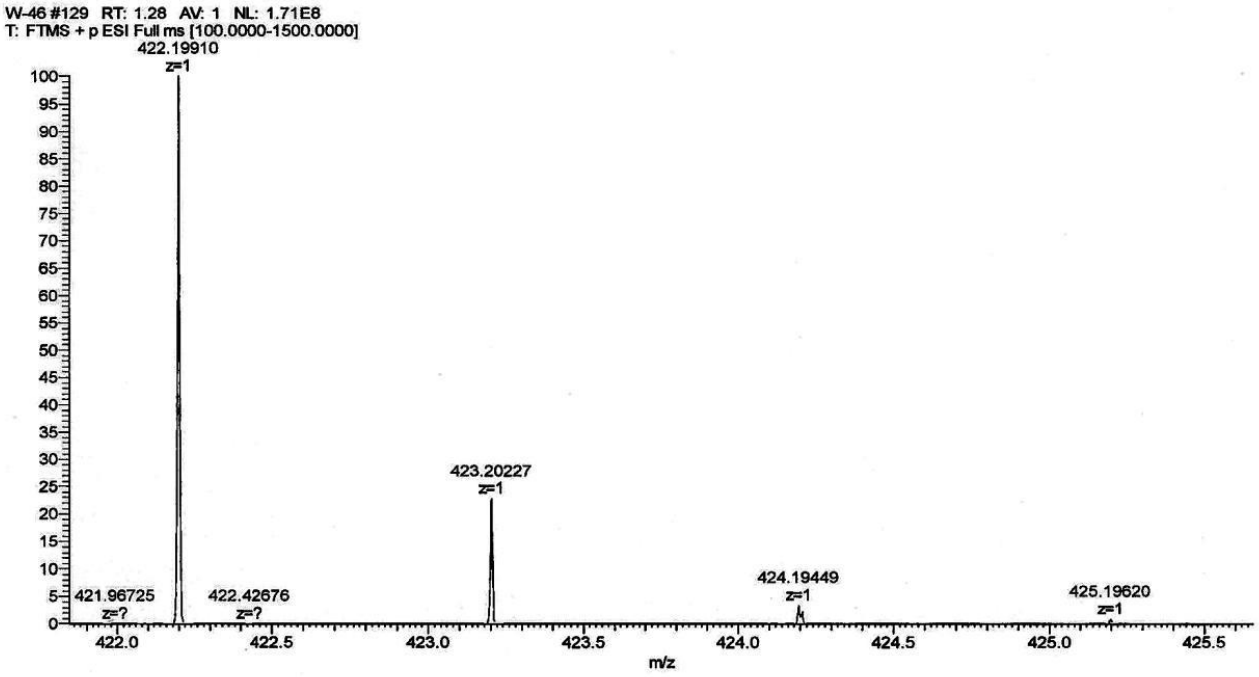

m/z	Theo. Mass	Delta (ppm)	RDB equiv.	Composition	
422.19910	422.19957	-1.11	7.5	C22 H32 O5 N S	M+H

Figure S10. (+)-HRESIMS of compound **1**.

Thermo Qexactive Focus Report

compound NO. : W-46

Method : LCMS(compound)-low

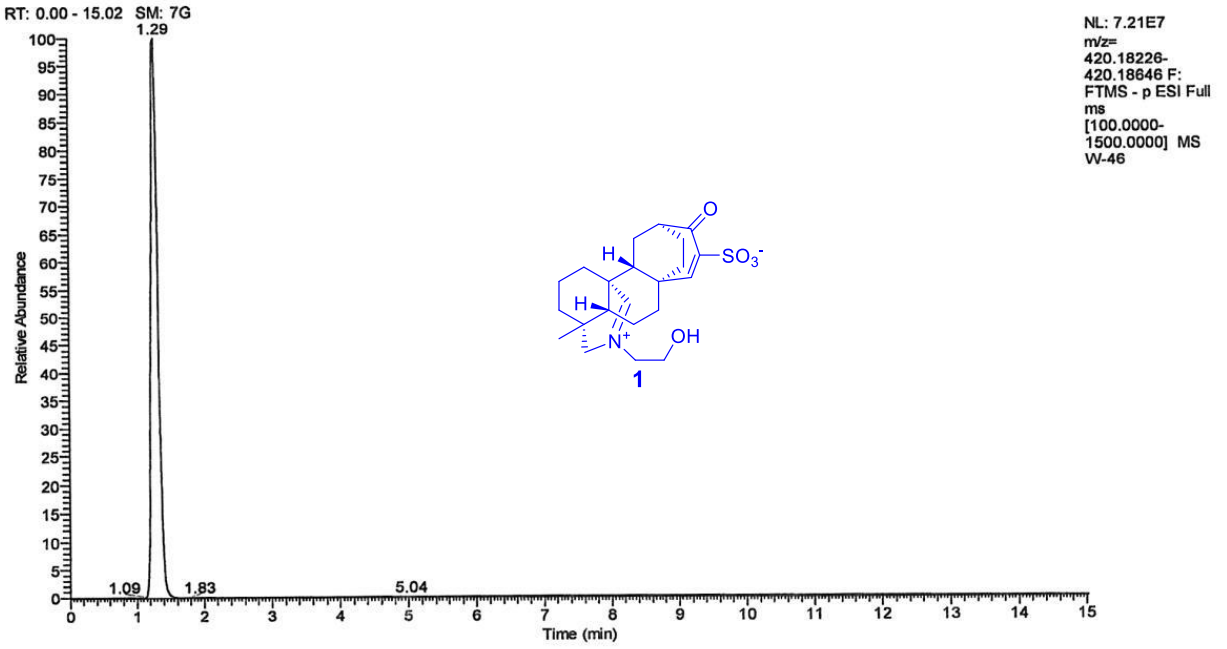

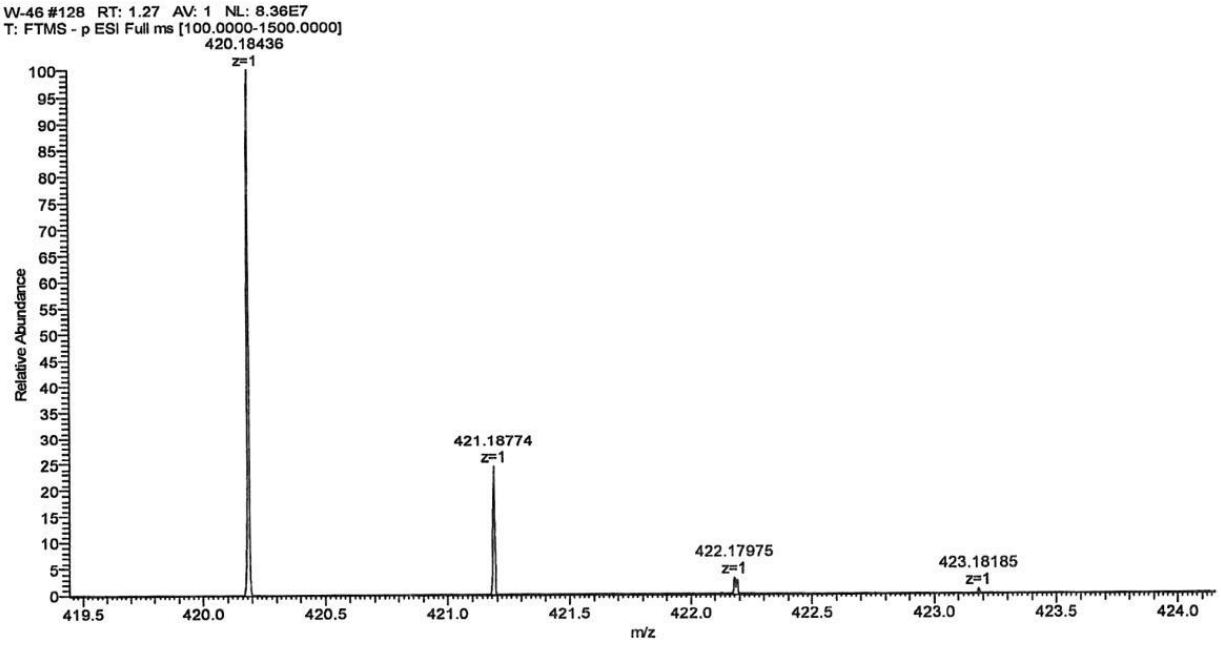

m/z	Theo. Mass	Delta (ppm)	RDB equiv.	Composition	
420.18436	420.18502	-1.56	8.5	C22 H30 O5 N S	M-H

Figure S11. (–)-HRESIMS of compound **1**.

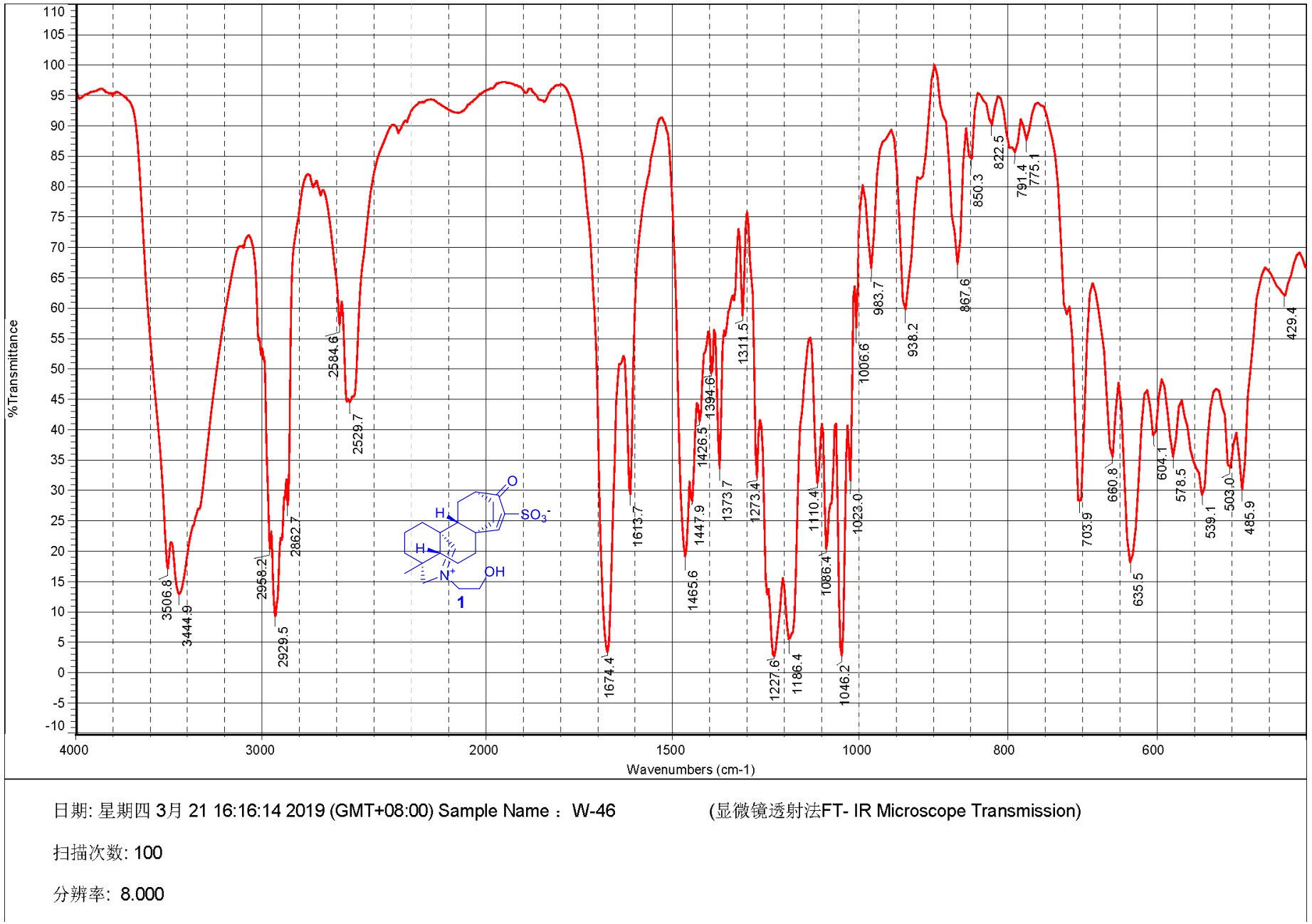

Figure S12. The IR spectrum of compound **1**.

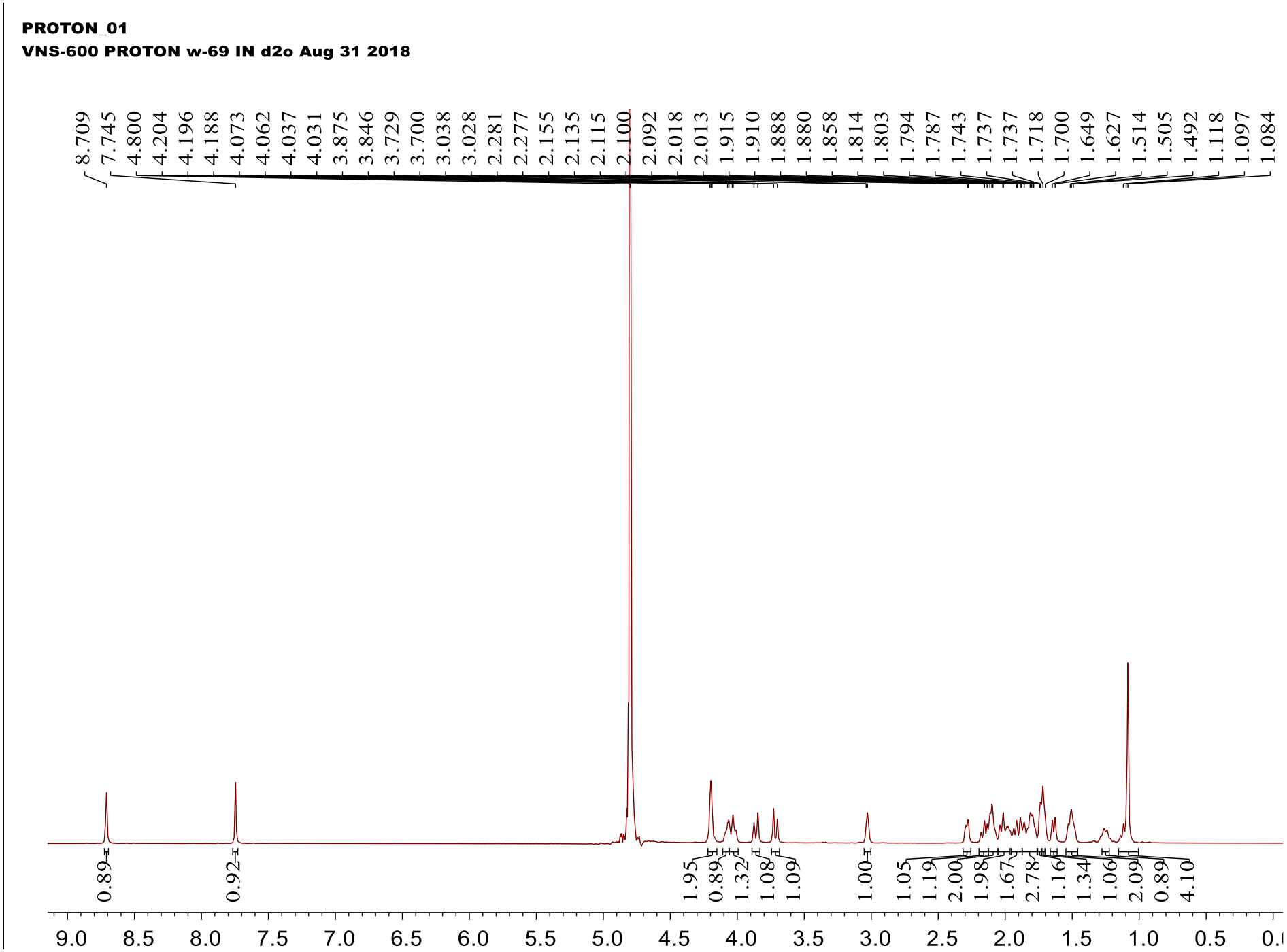

Figure S13. The ^{1}H NMR spectrum of compound **1** in D_2O (600 MHz).

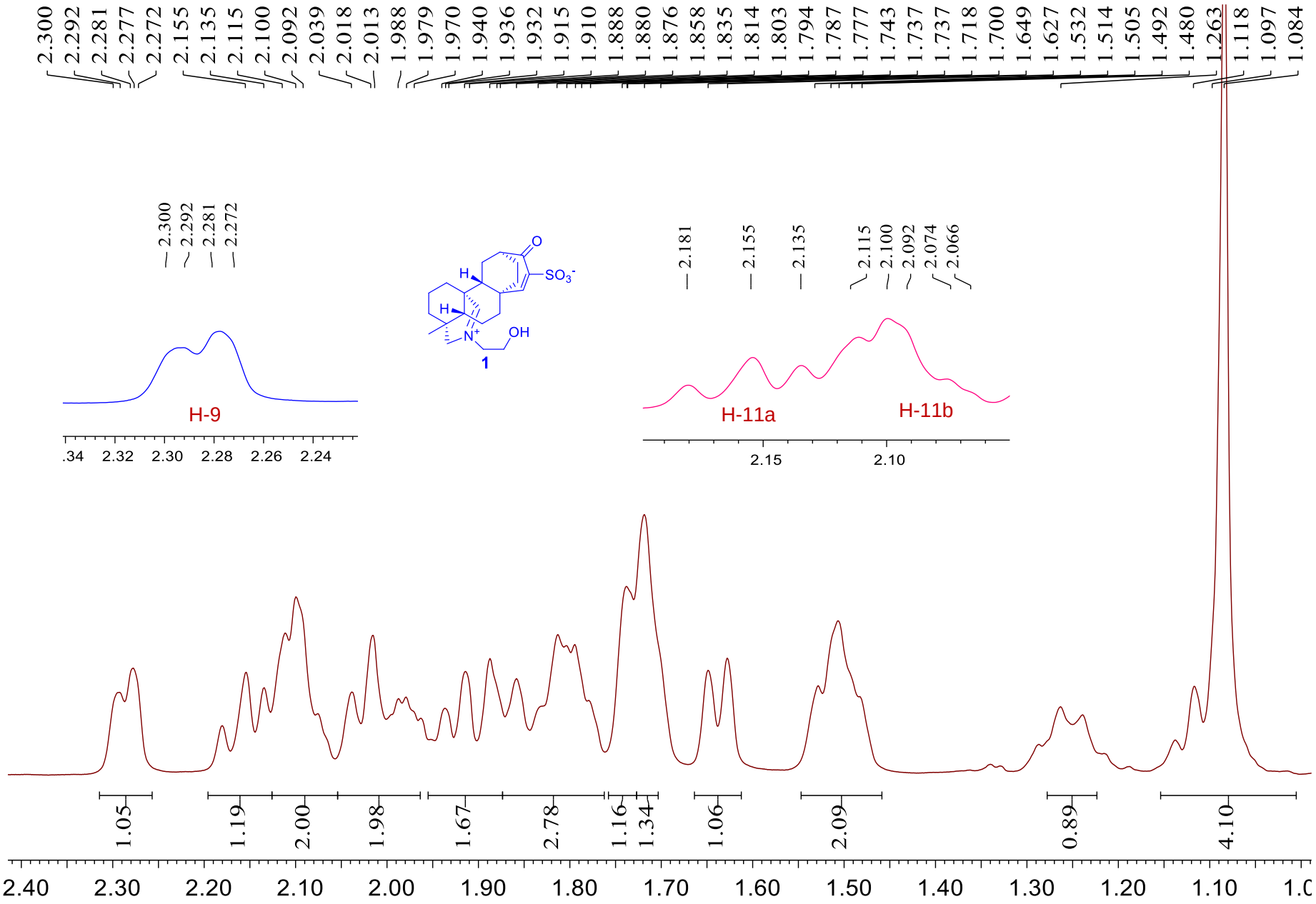

Figure S14. An expansion of the 1–2.4 ppm region of the ^{1}H NMR spectrum of compound **1** in D_2O (600 MHz).

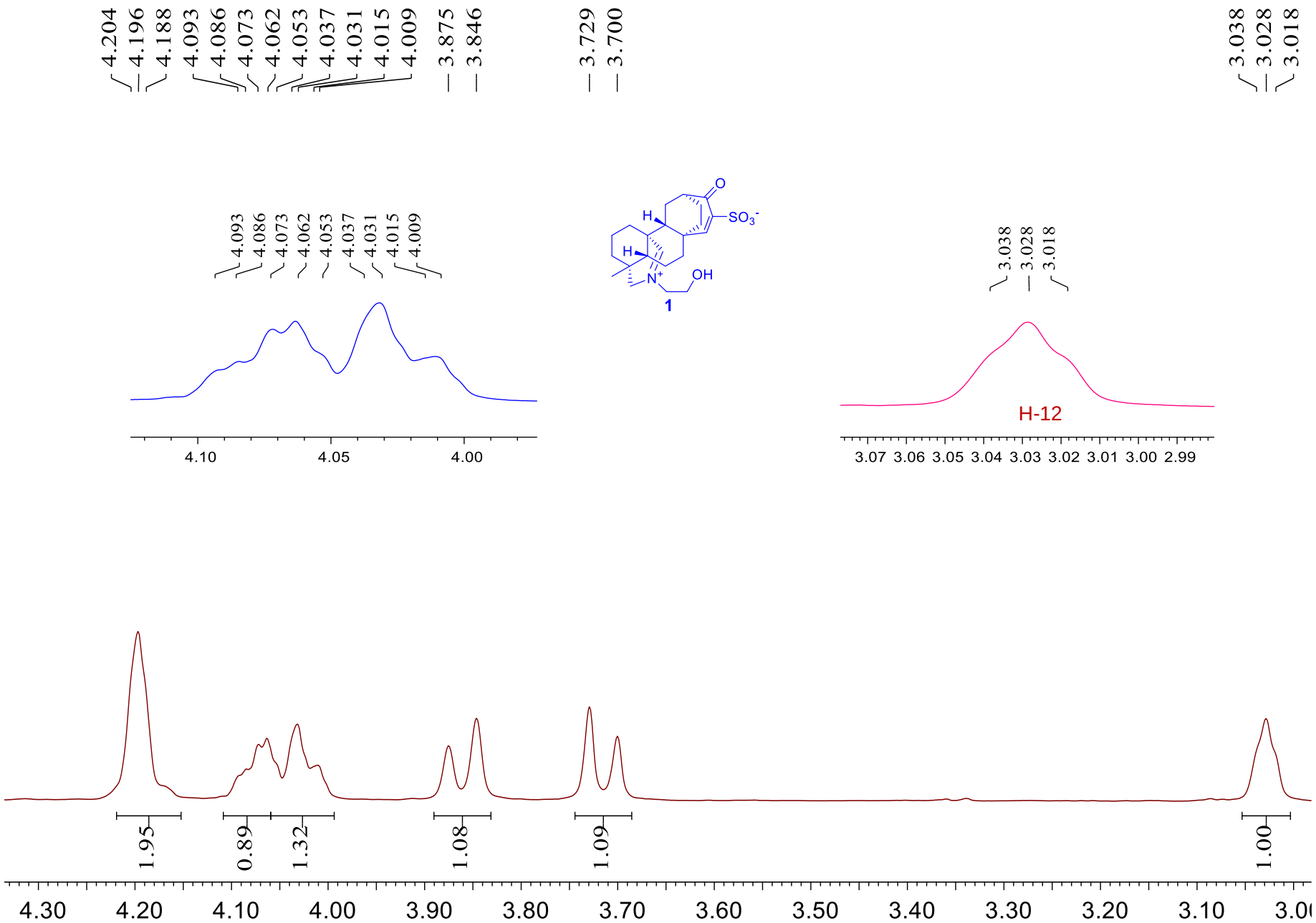

Figure S15. An expansion of the 3.0–4.3 ppm region of the ^{1}H NMR spectrum of compound **1** in D_2O (600 MHz).

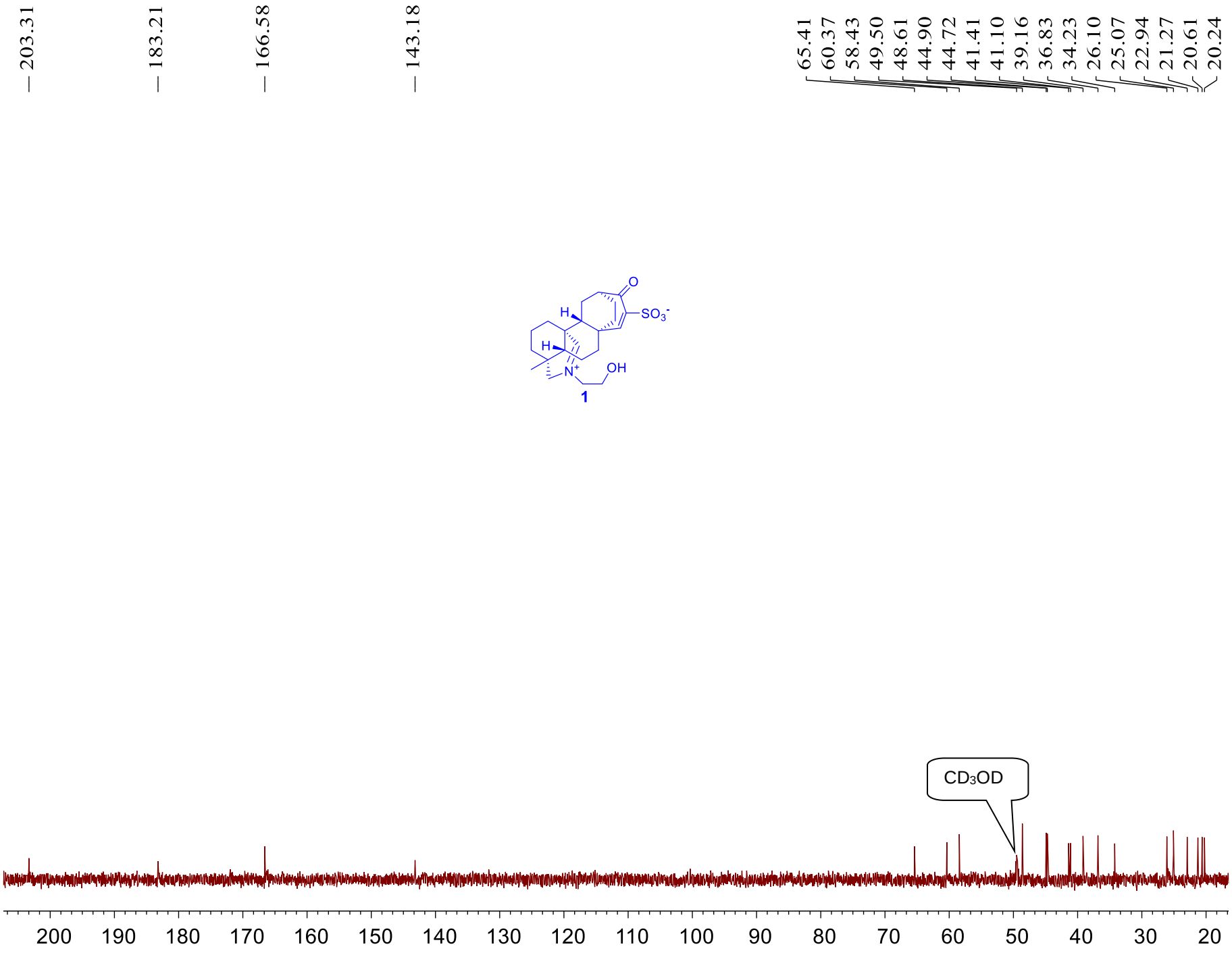

Figure S16. The ^{13}C NMR spectrum of compound **1** in D_2O (150 MHz).

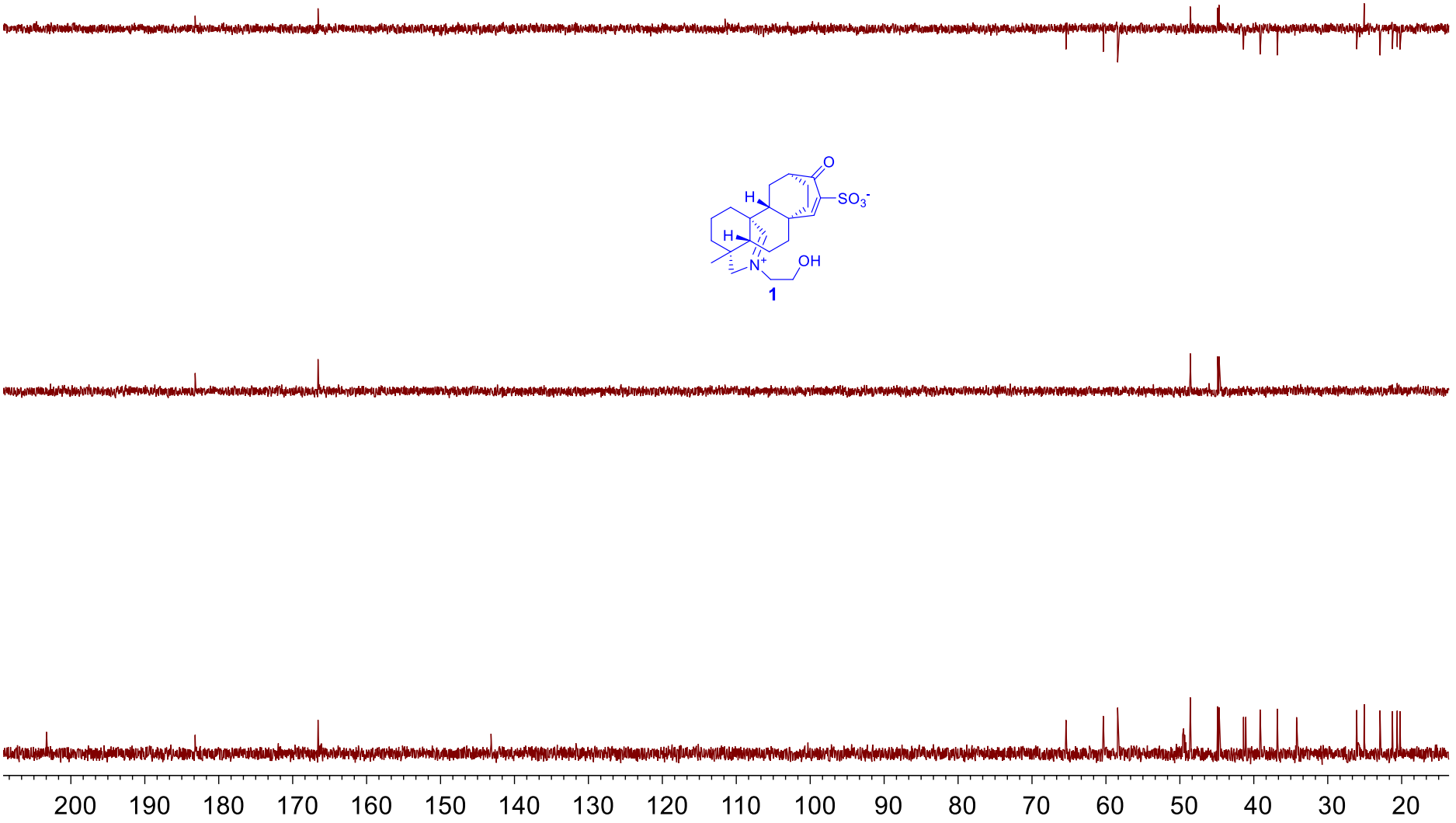

Figure S17. The DEPT spectrum of compound **1** in D_2O (150 MHz).

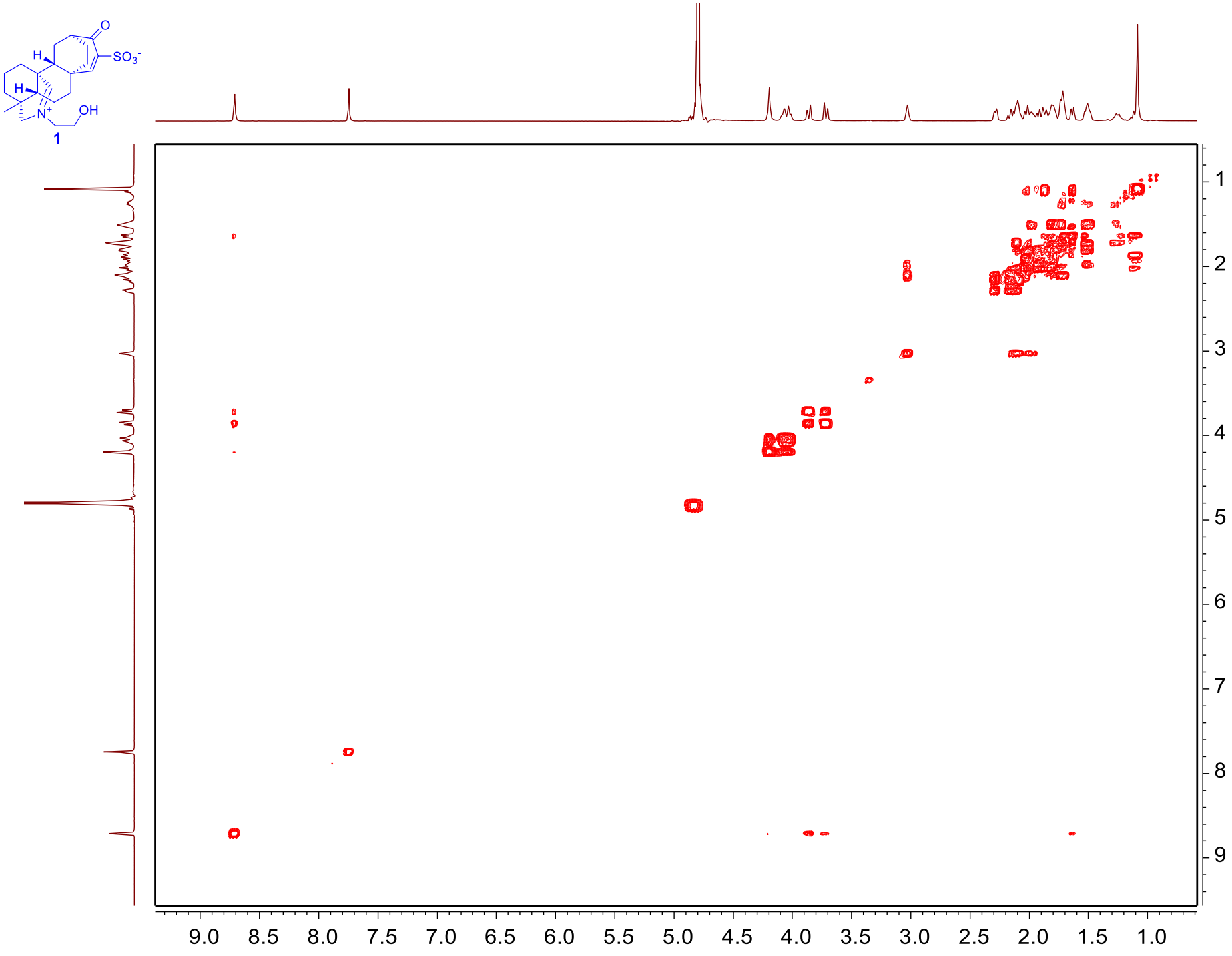

Figure S18. The ^{1}H-^{1}H COSY spectrum of compound **1** in D_2O (600 MHz).

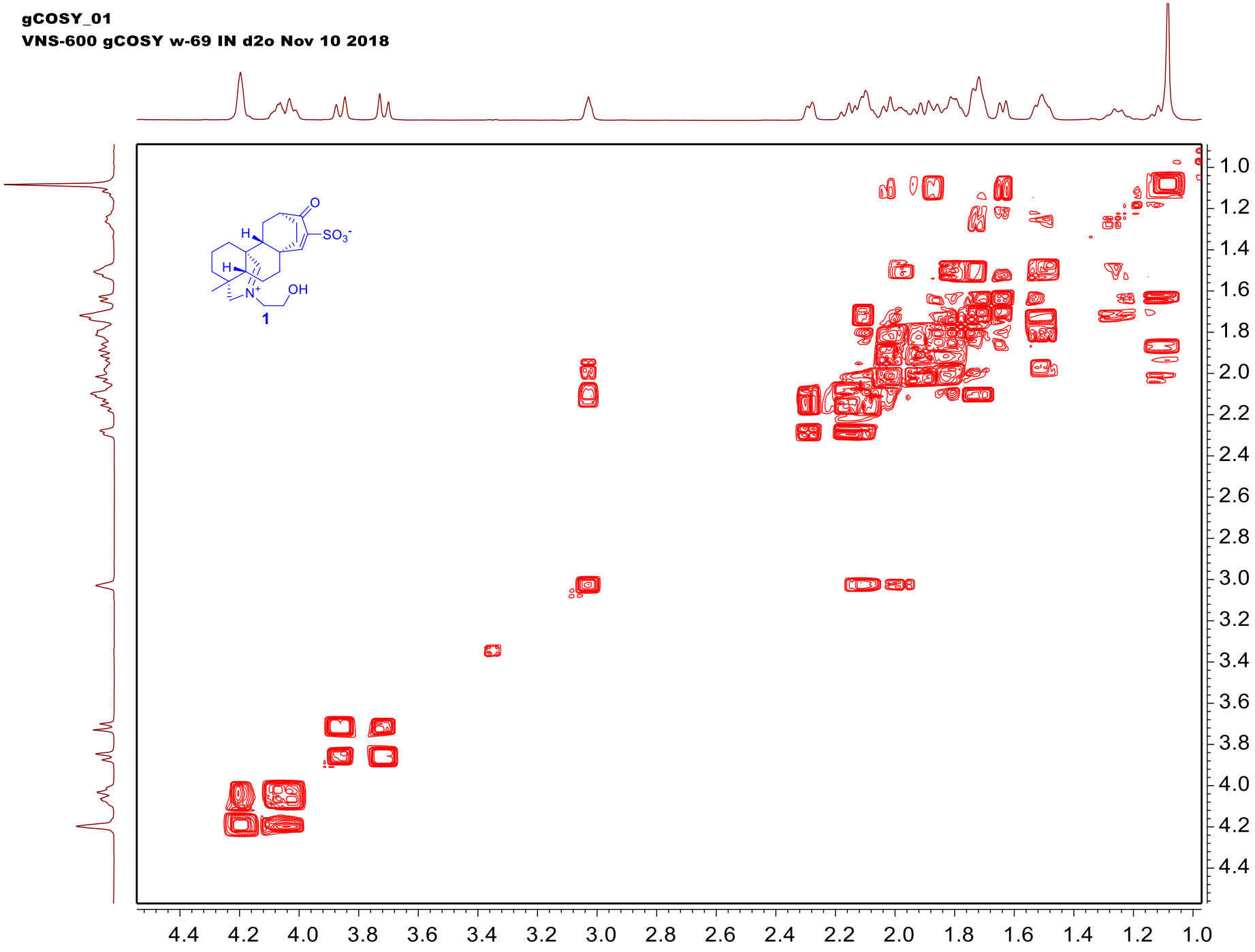

Figure S19. An expansion of 1.0–4.4 ppm region of the ^{1}H-^{1}H COSY spectrum of compound **1** in D_2O (600 MHz).

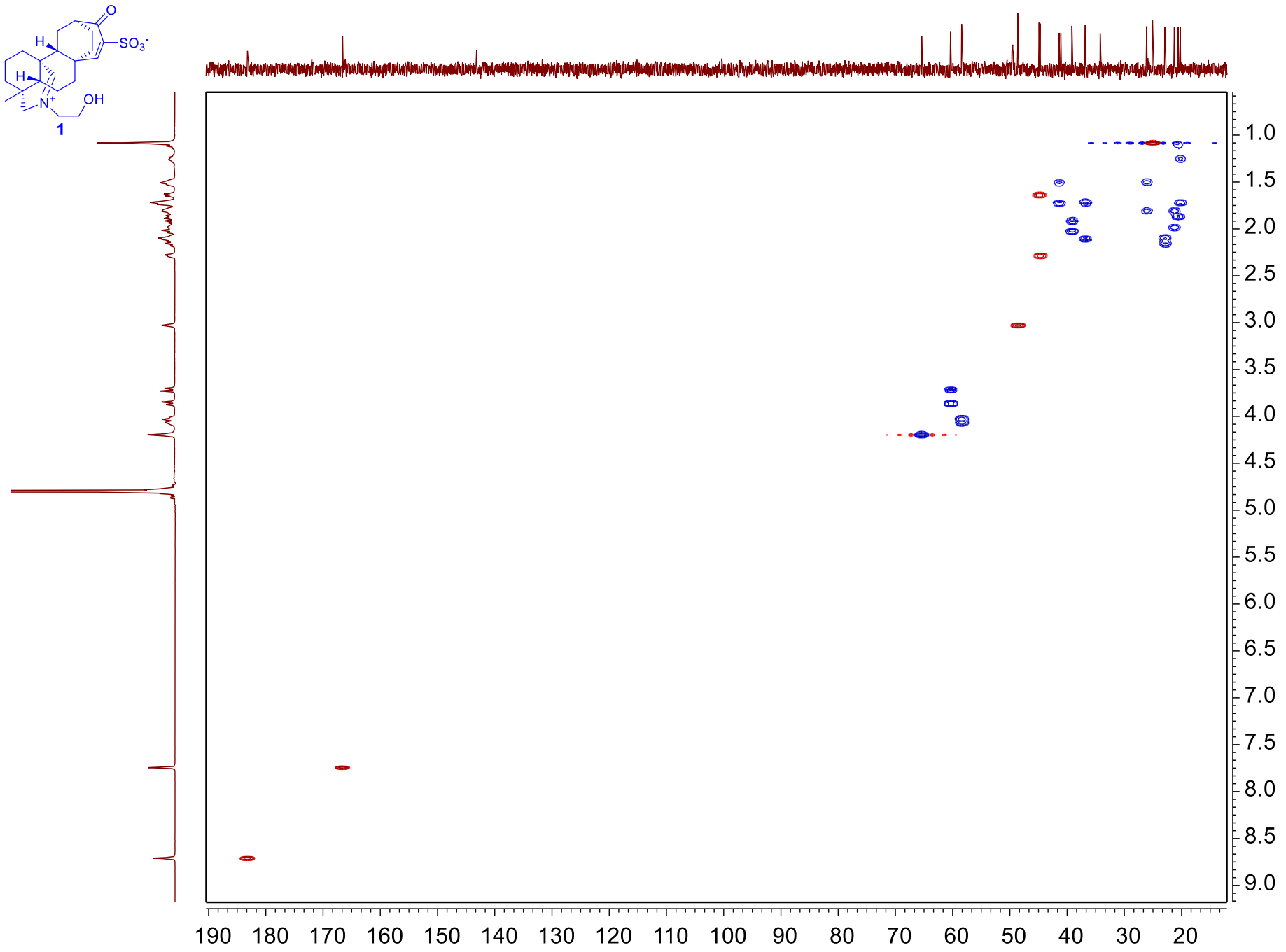

Figure S20. The HSQC spectrum of compound **1** in D_2O (600 MHz for ^1H).

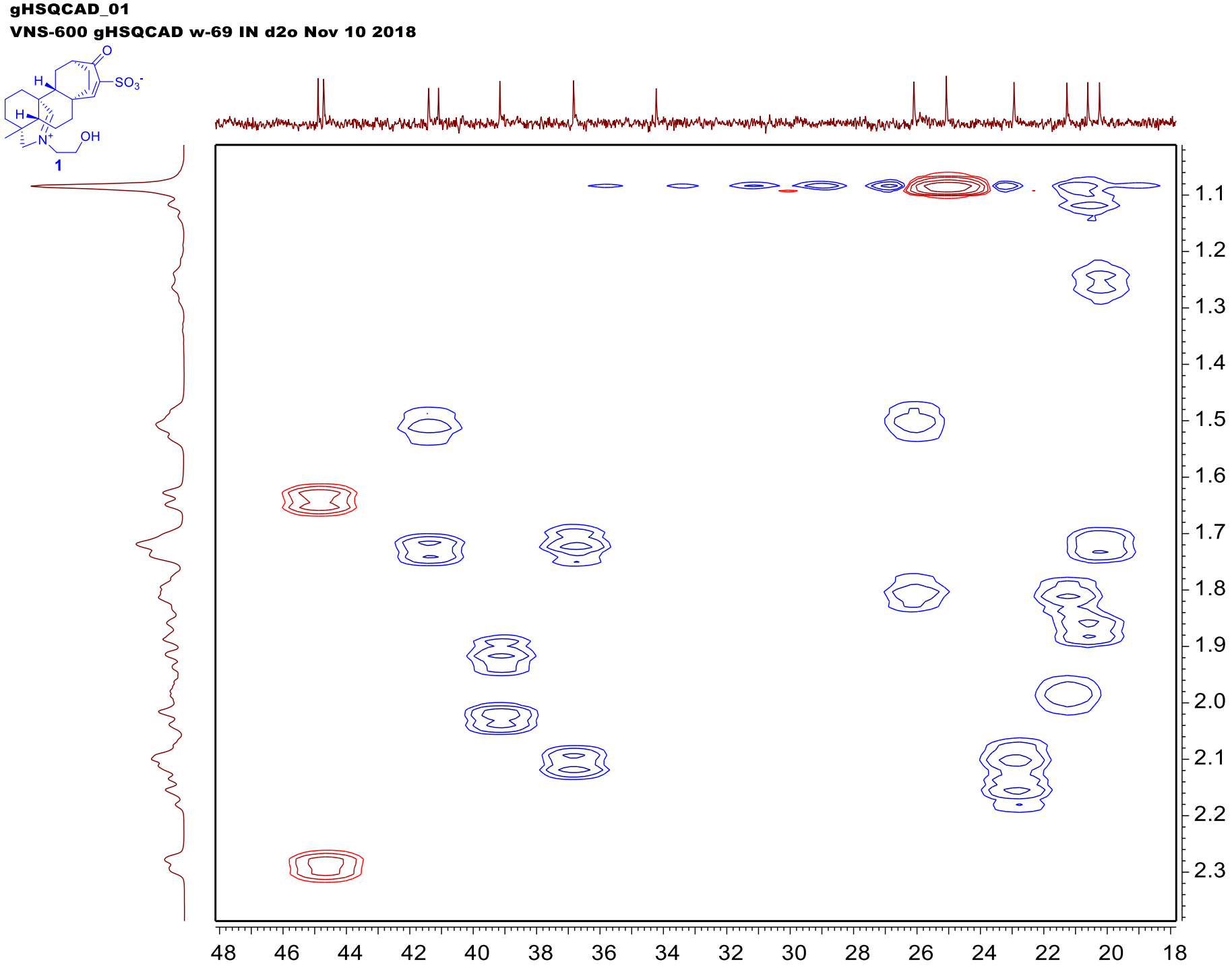

Figure S21. An expansion of the 1.0–2.4 (^{1}H)/18–48 (^{13}C) ppm region (^{1}H) of the HSQC spectrum of compound **1** in D_2O (600 MHz for ^{1}H).

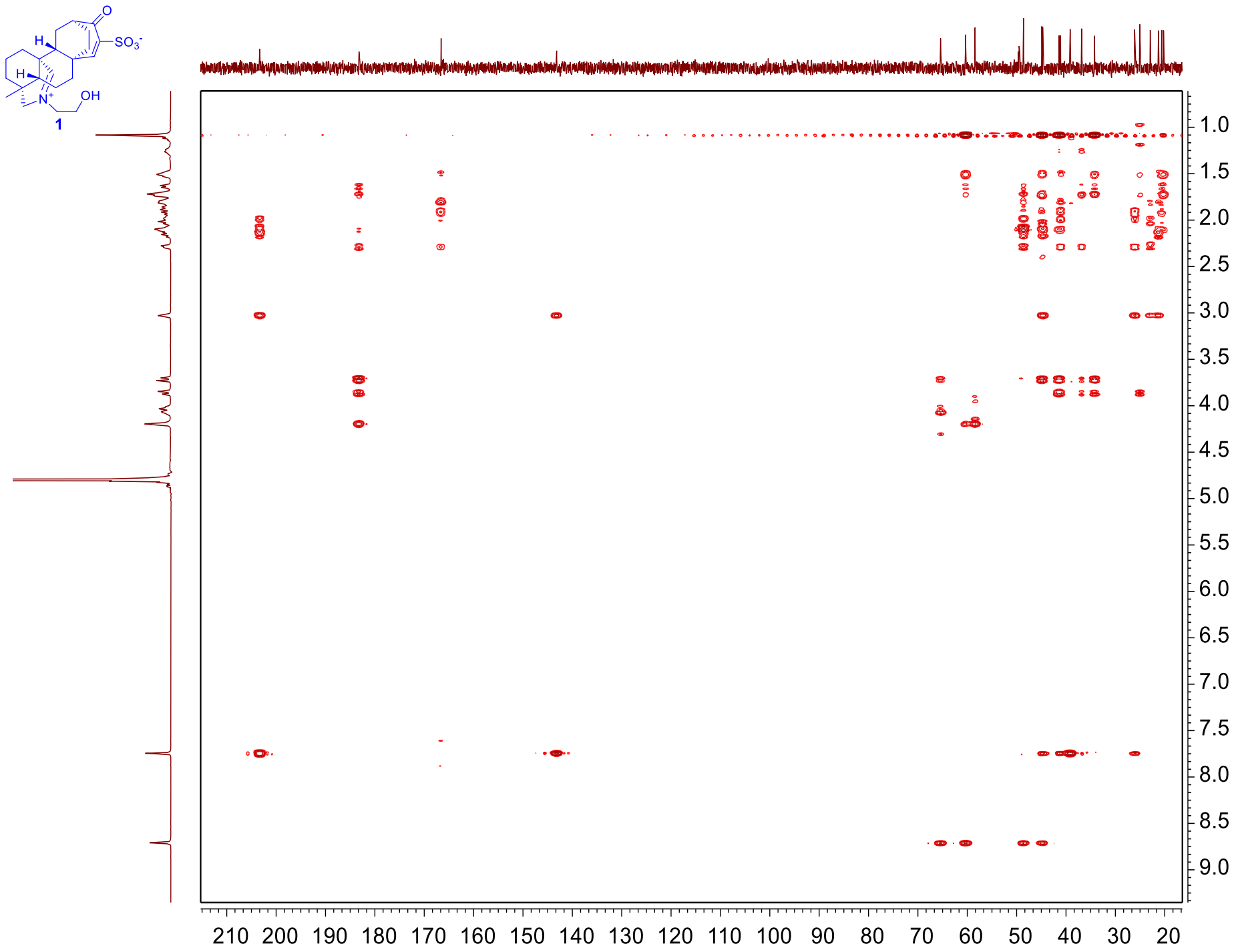

Figure S22. The HMBC spectrum of compound **1** in D_2O (600 MHz for ^1H).

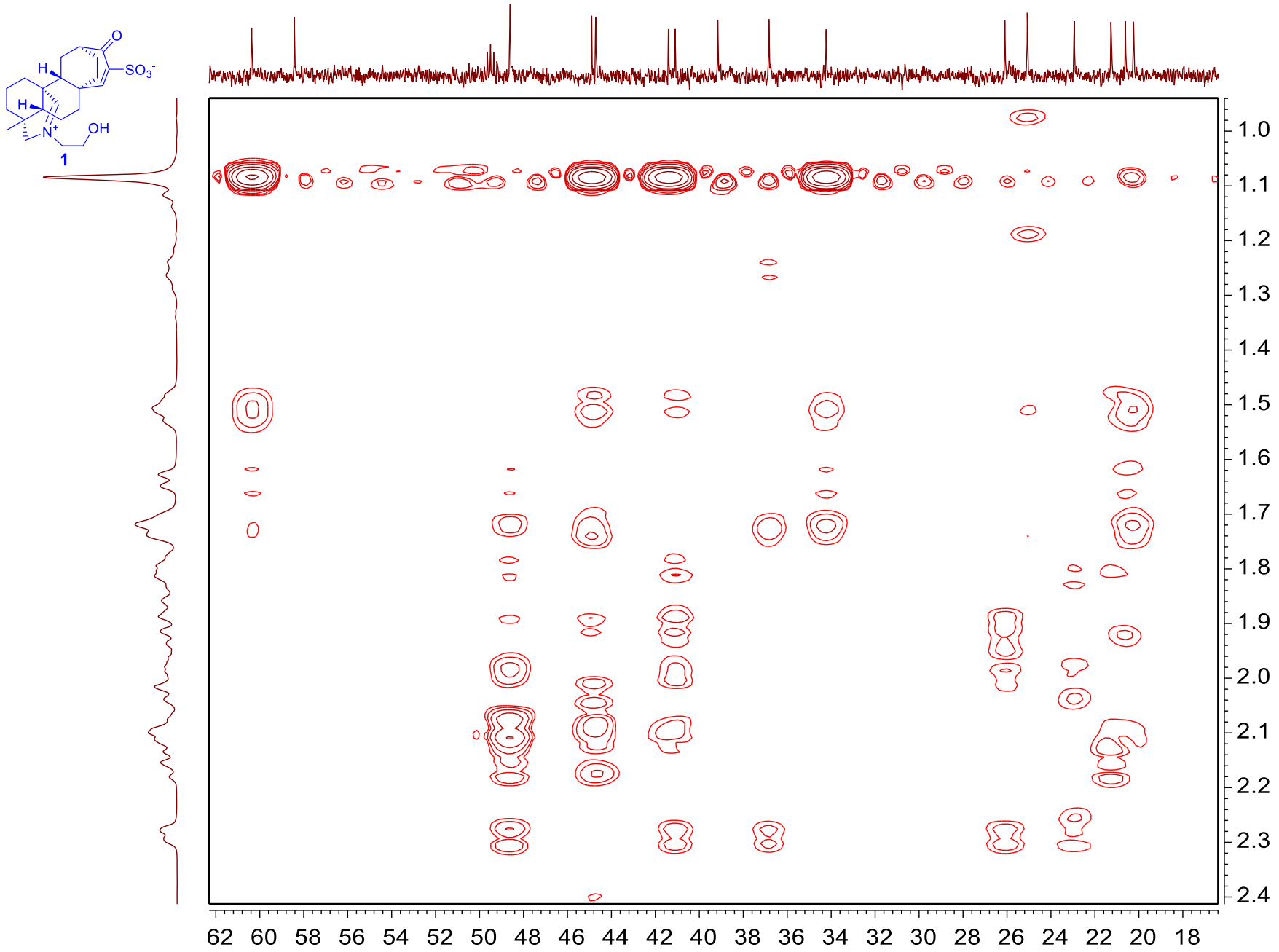

Figure S23. An expansion of the 1.0–2.4 (^{1}H)/18–62 (^{13}C) ppm region of the HMBC spectrum of compound **1** in D_2O (600 MHz for ^{1}H).

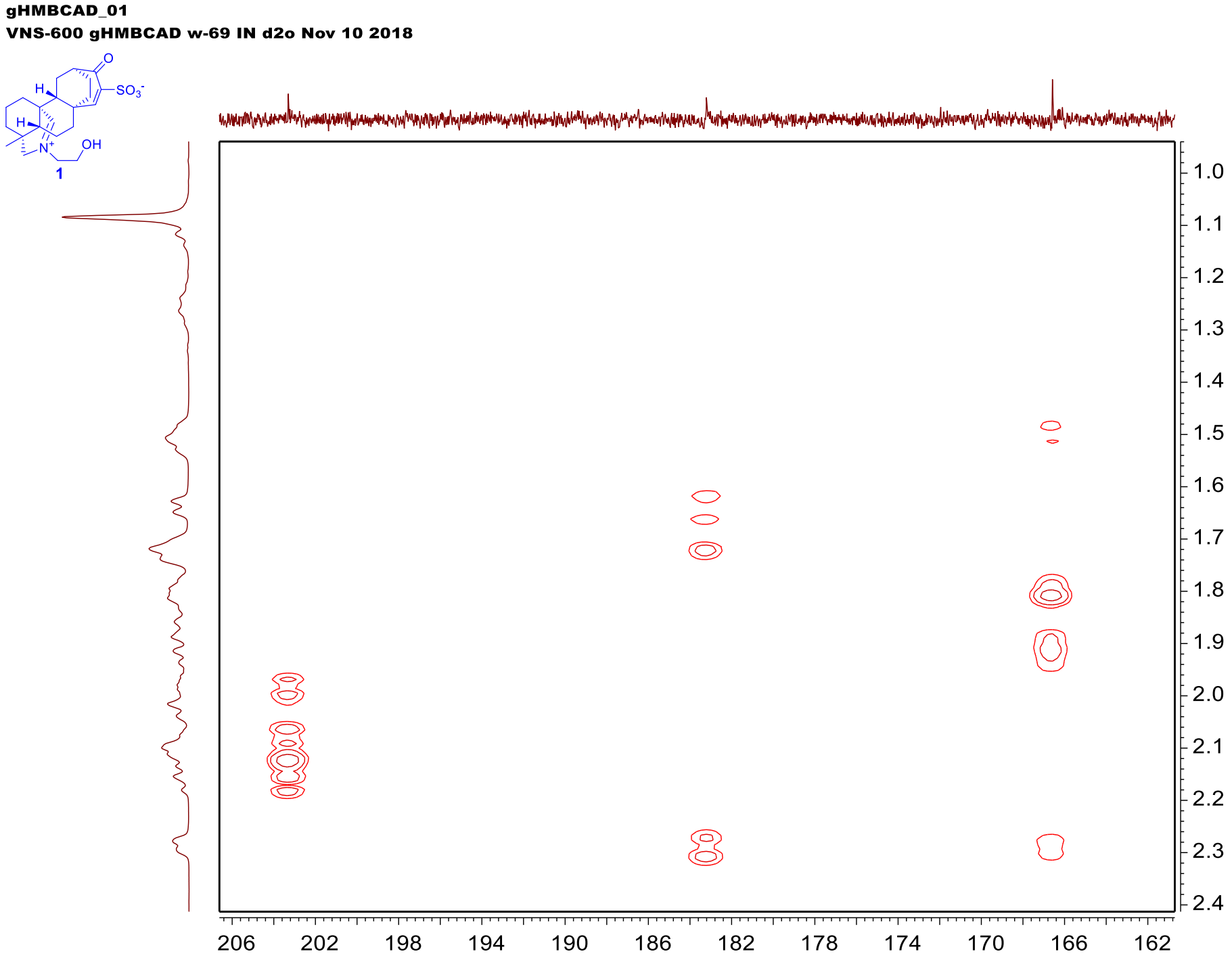

Figure S24. An expansion of the 1.0–2.4 (^{1}H)/162–206 (^{13}C) ppm region of the HMBC spectrum of compound **1** in D_2O (600 MHz for ^{1}H).

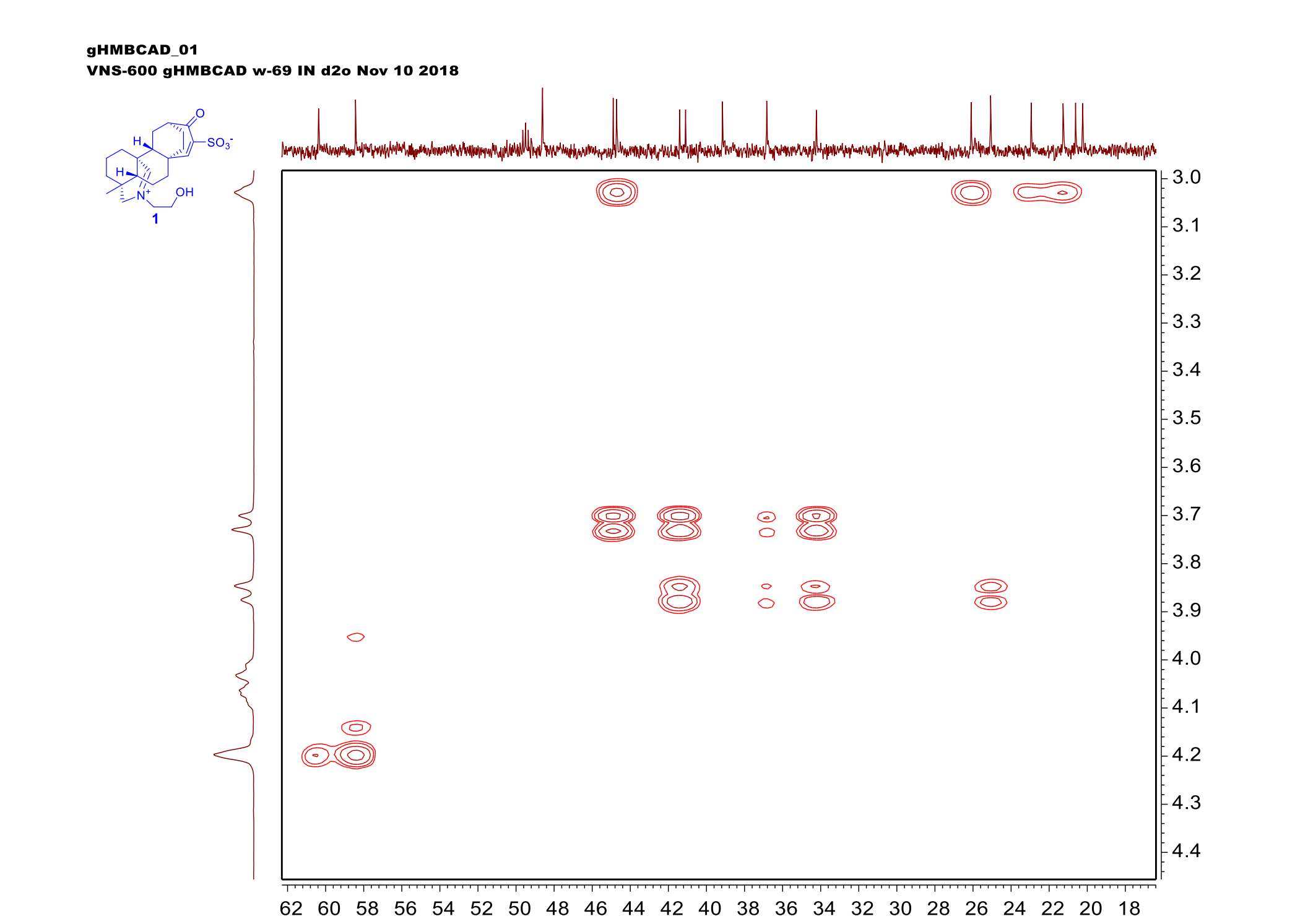

Figure S25. An expansion of the 3.0–4.5 (^{1}H)/18–62 (^{13}C) ppm region of the HMBC spectrum of compound **1** in D_2O (600 MHz for ^{1}H).

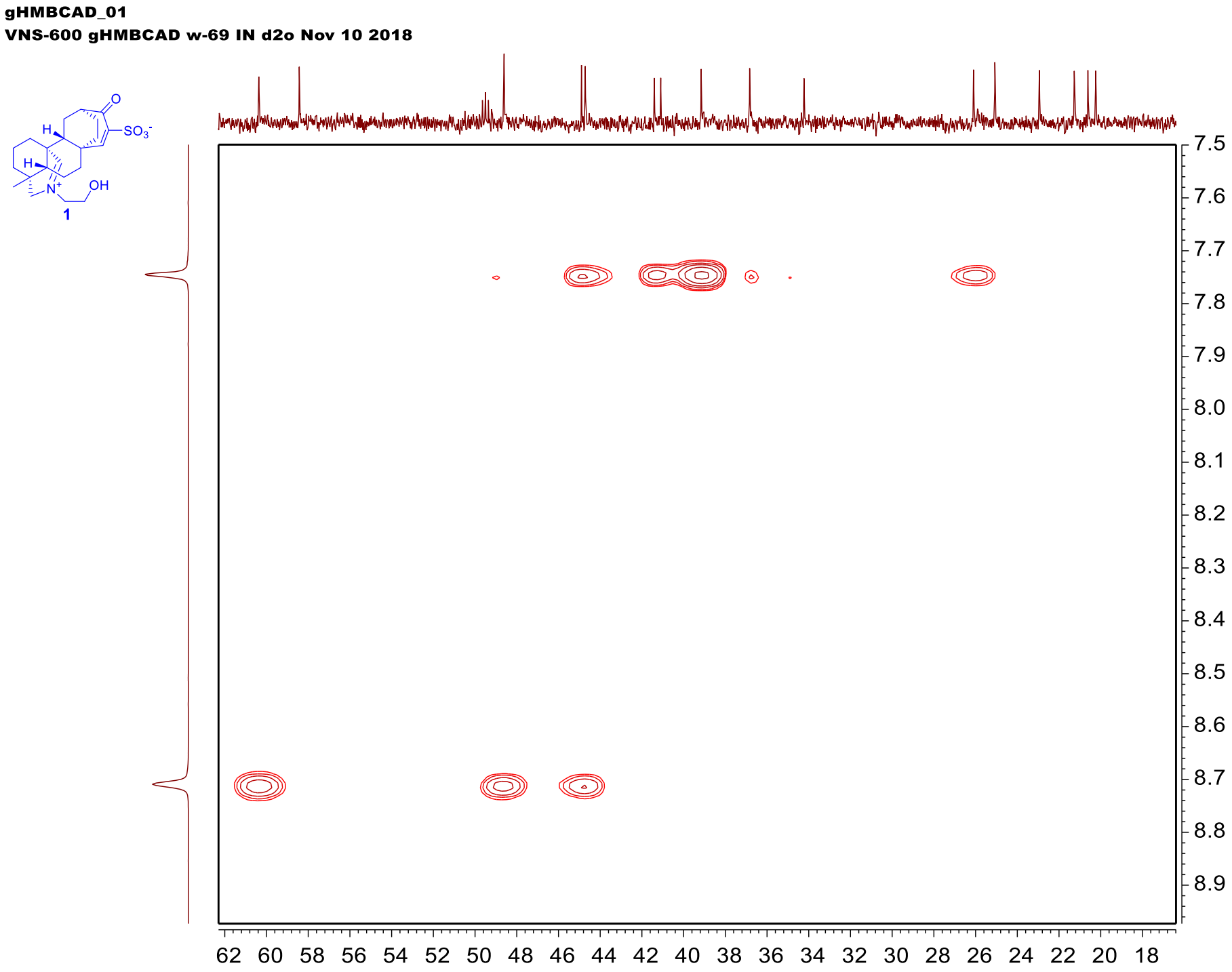

Figure S26. An expansion of the 7.5–9.0 (^{1}H)/18–62 (^{13}C) ppm region of the HMBC spectrum of compound **1** in D_2O (600 MHz for ^{1}H).

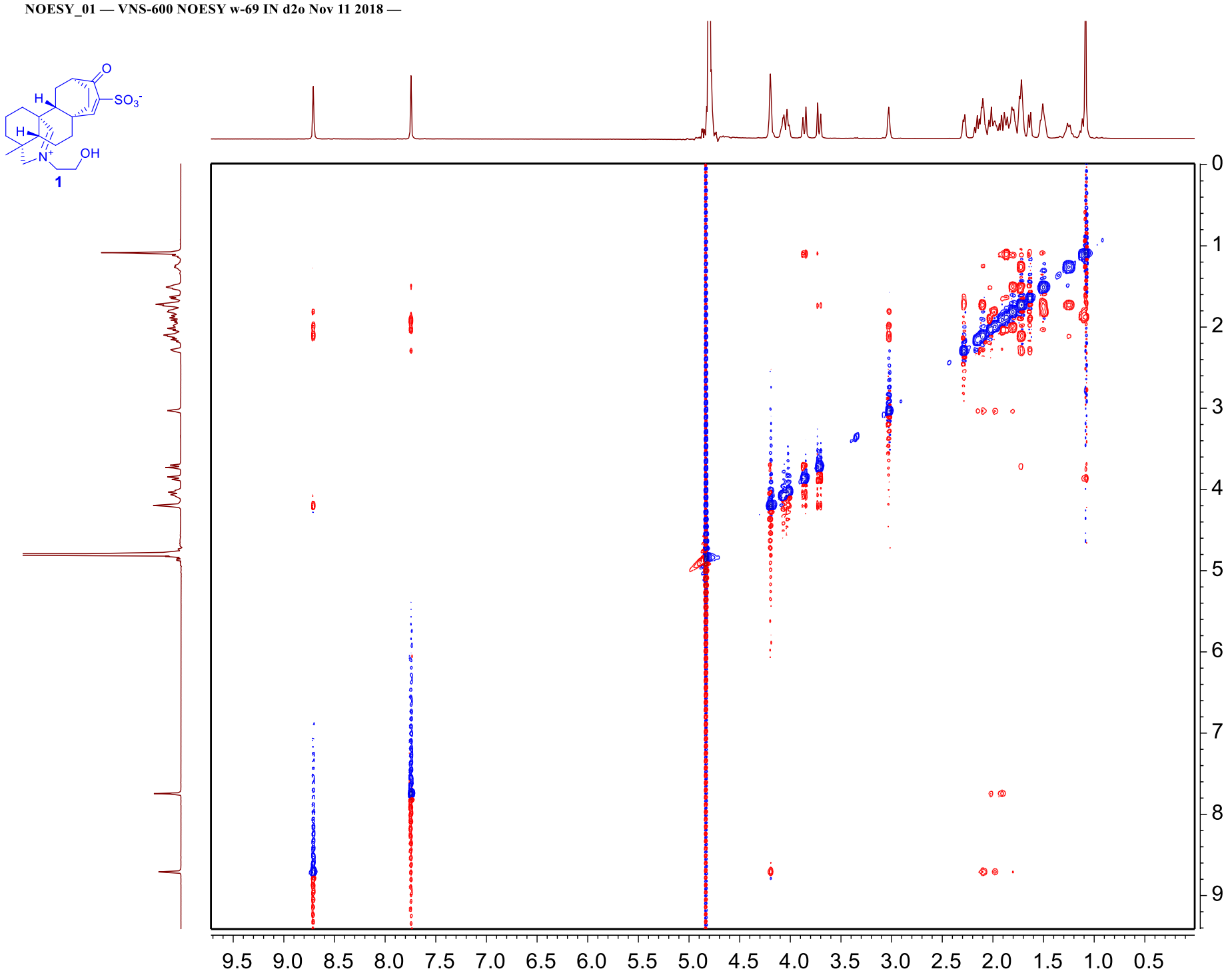

Figure S27. The NOESY spectrum of compound **1** in D_2O (600 MHz).

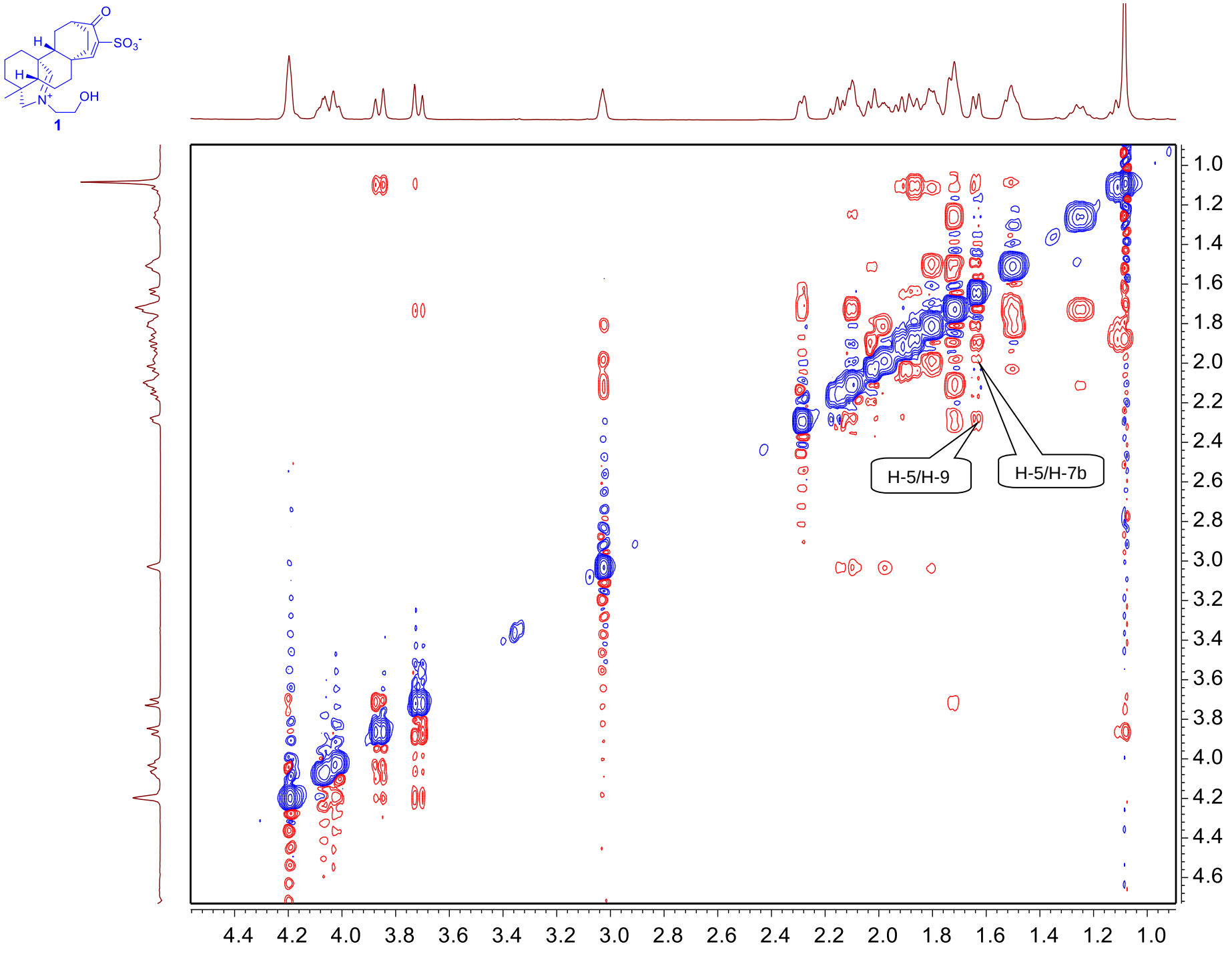

Figure S28. An expansion of 1–4.5 ppm region of the NOESY spectrum of compound **1** in D_2O (600 MHz).

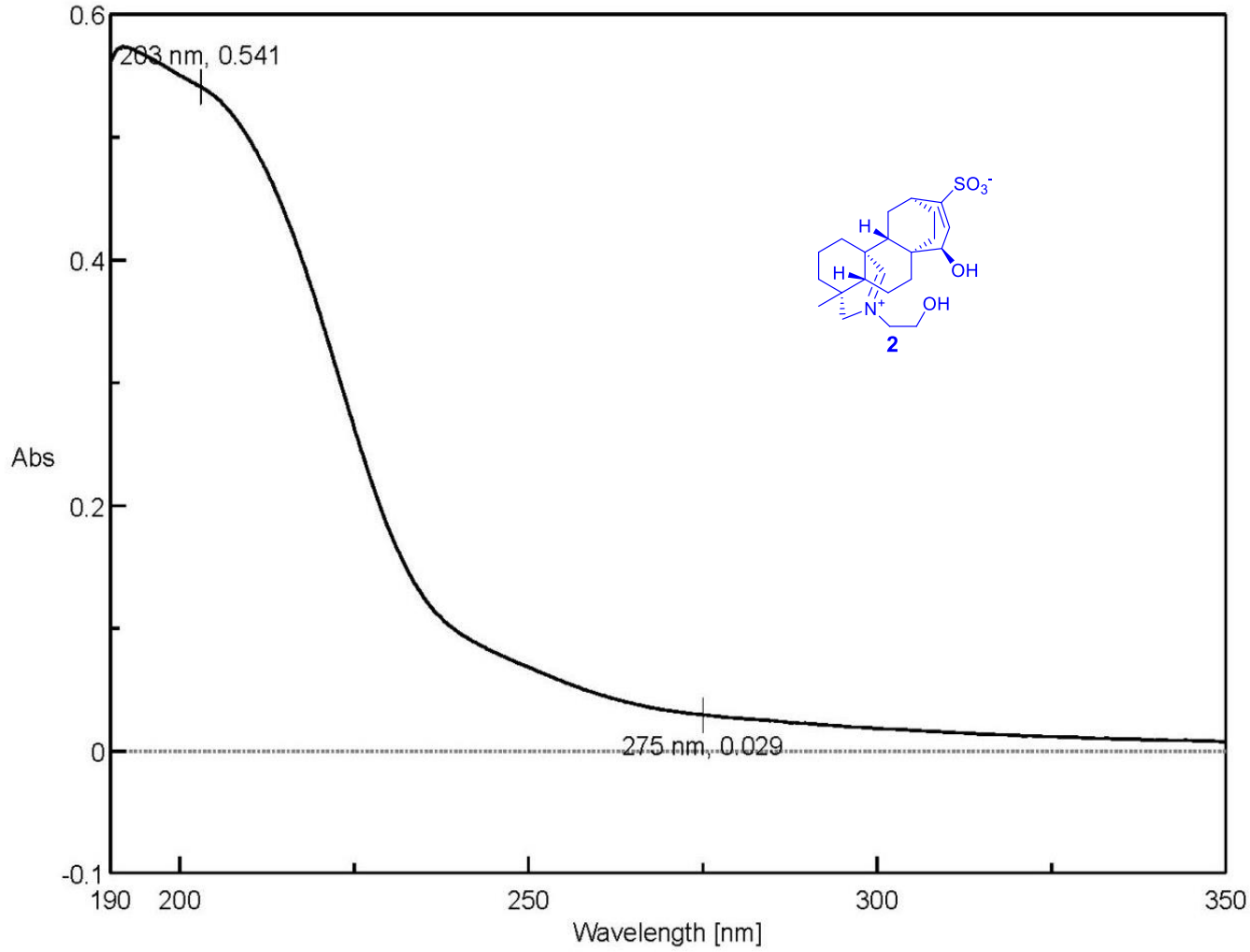

[Comment]
Sample Name 3-4-6
Comment
User
Division UV
Company
[Measurement Information]
Instrument Name V-650
Model Name V-650
Serial No. A034461150

Accessory PSC-718
Accessory S/N A001761114
Position 2
Cell Length 10 mm
Temperature 20.01 C
Control Sonsor Holder
Monitor Sensor Holder
Start Mode Start immediately

Photometric Mode Abs
Measurement range 600 - 190 nm
Data pitch 0.2 nm
Band width(UV/Vis) 2.0 nm
Response Medium
Scanning speed 200 nm/min
Source Change 340 nm
Light Source D2/WI
Filter Exchange Step
Correction Baseline

3-4-6

[Data Information]
Creation Date 2019-4-17 16:01

Data array type Linear data array
Horizontal Wavelength [nm]
Vertical Abs
Start 600 nm
End 190 nm
Data pitch 0.2 nm
Data points 2051

Figure S29. The UV spectrum of **2** in H_2O.

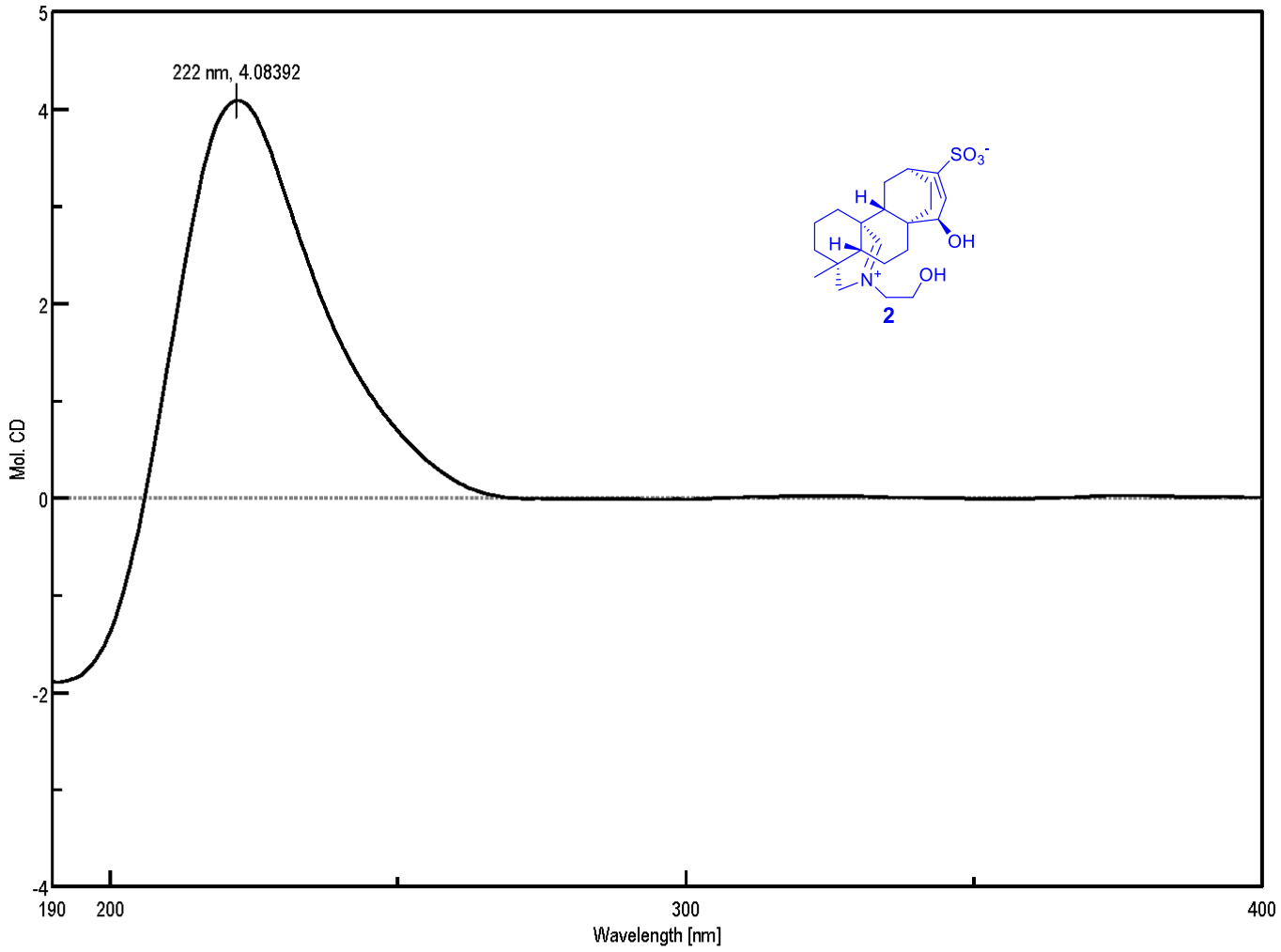

[Measurement Information]

Instrument Name	J-815
Model Name	J-815
Serial No.	A024461168
Accessory	Standard
Accessory S/N	A024461168
Cell Length	1 mm
Measurement date	2019/4/17 10:03
Photometric Mode	CD, HT, Abs
Measure Range	400 - 190 nm
Data pitch	0.5 nm
Sensitivity	Standard
D.I.T.	1 sec
Bandwidth	1.00 nm
Start Mode	Immediately
Scanning Speed	100 nm/min
Baseline Correction	Baseline
Shutter Control	Auto
CD Detector	PMT
PMT Voltage	Auto
Accumulations	2
Solvent	H2O
Concentration	0.8 (w/v)%

Figure S30. The CD spectrum of **2** in H_2O.

Thermo Qexactive Focus Report

compound NO. : W 3-4-6

Method : LCMS(compound)-low

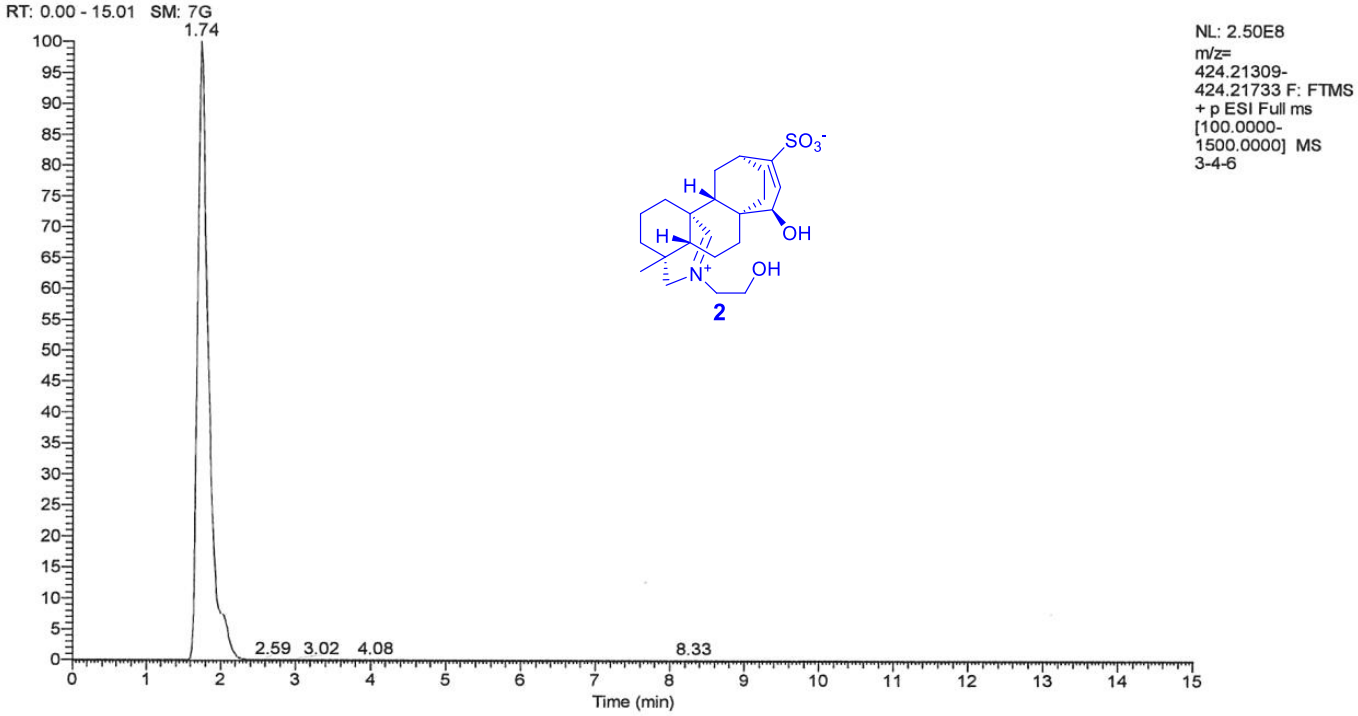

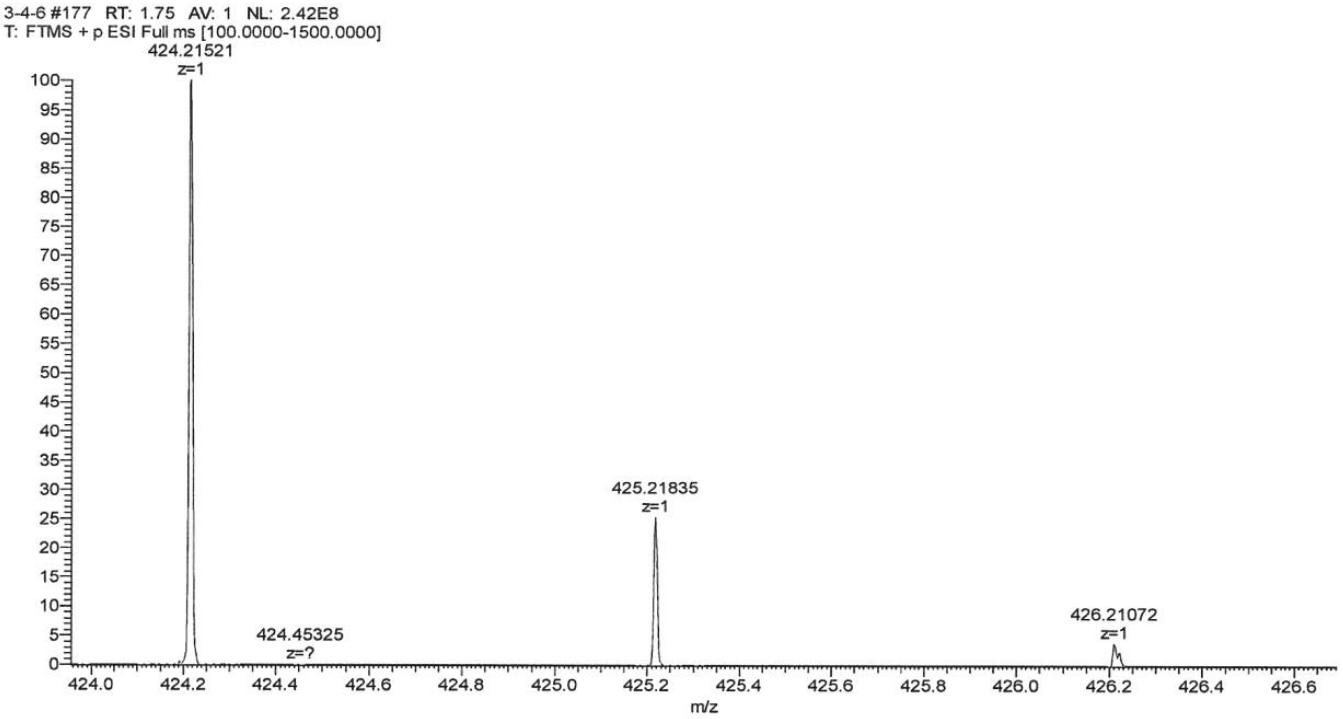

m/z	Theo. Mass	Delta (ppm)	RDB equiv.	Composition	
424.21521	424.21522	-0.02	6.5	C22 H34 O5 N S	M+H

Figure S31. (+)-HRESIMS report of **2**.

Thermo Qexactive Focus Report

compound NO. : 3-4-6

Method : LCMS(compound)-low

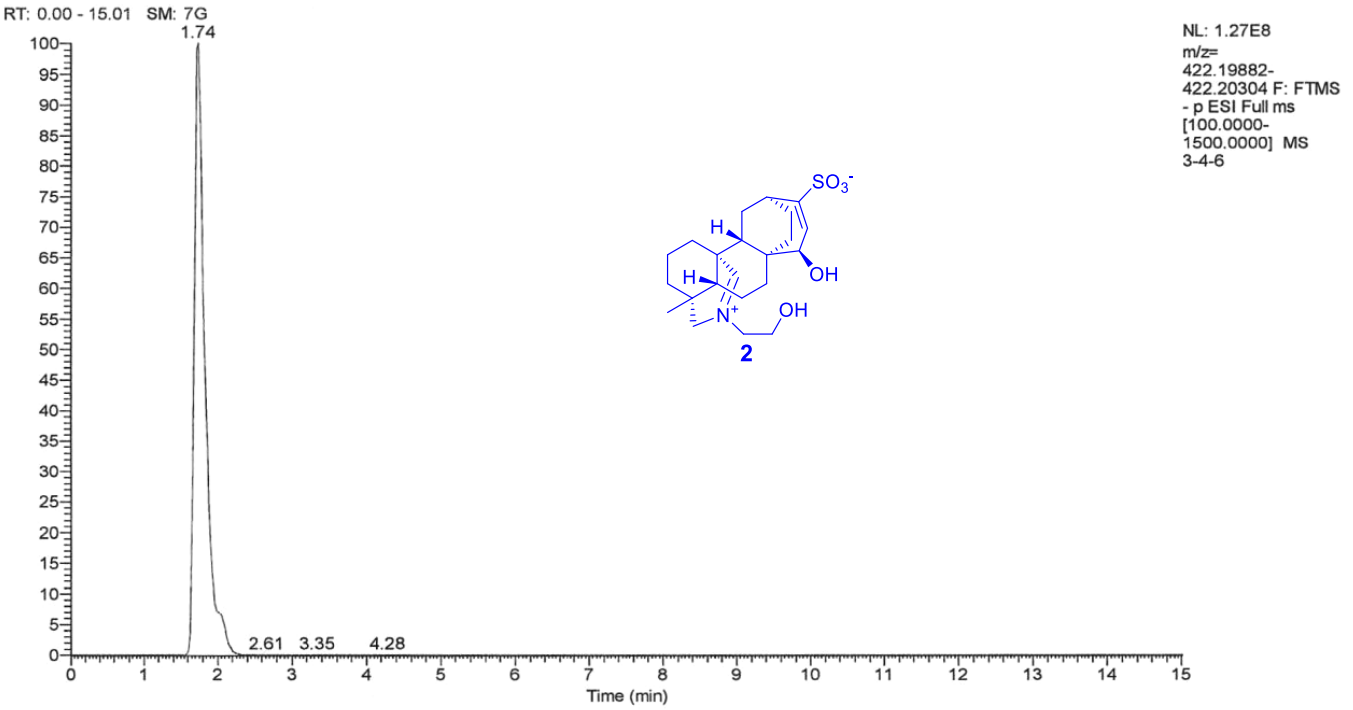

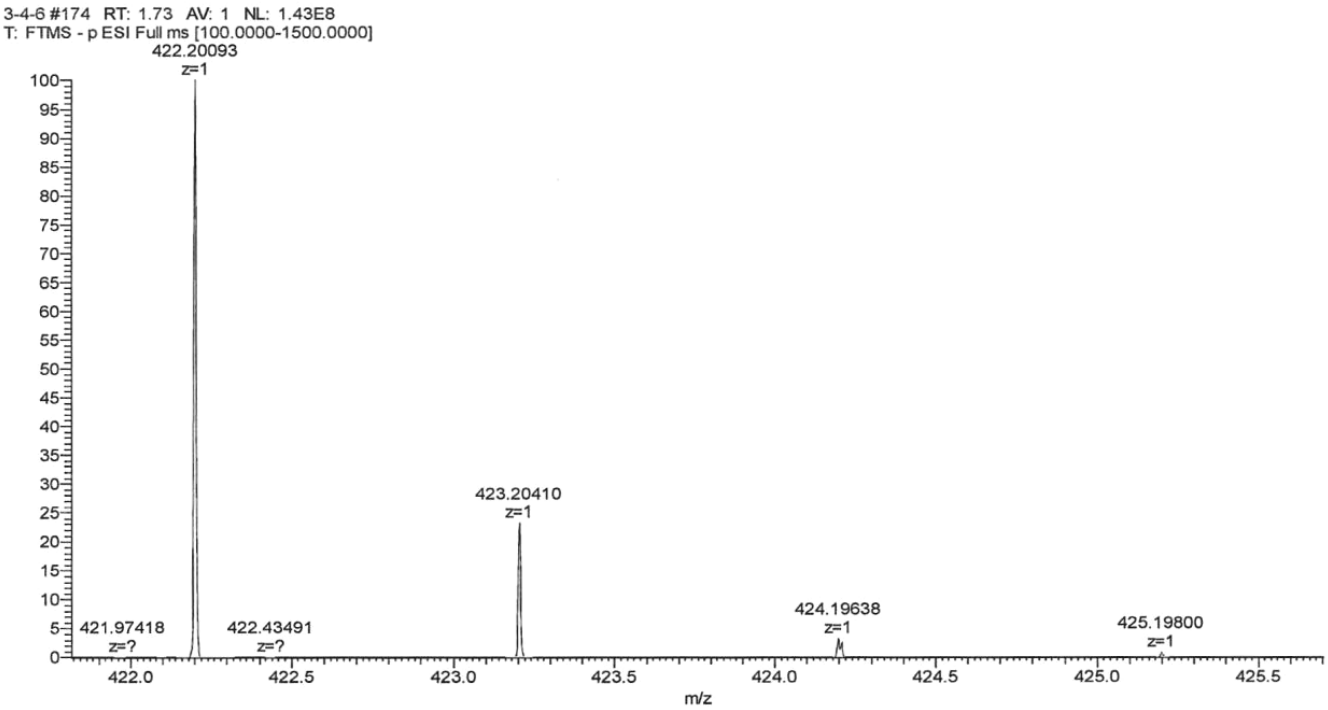

m/z	Theo. Mass	Delta (ppm)	RDB equiv.	Composition	
422.20093	422.20067	0.62	7.5	C22 H32 O5 N S	M-H

Figure S32. (–)-HRESIMS report of **2.**

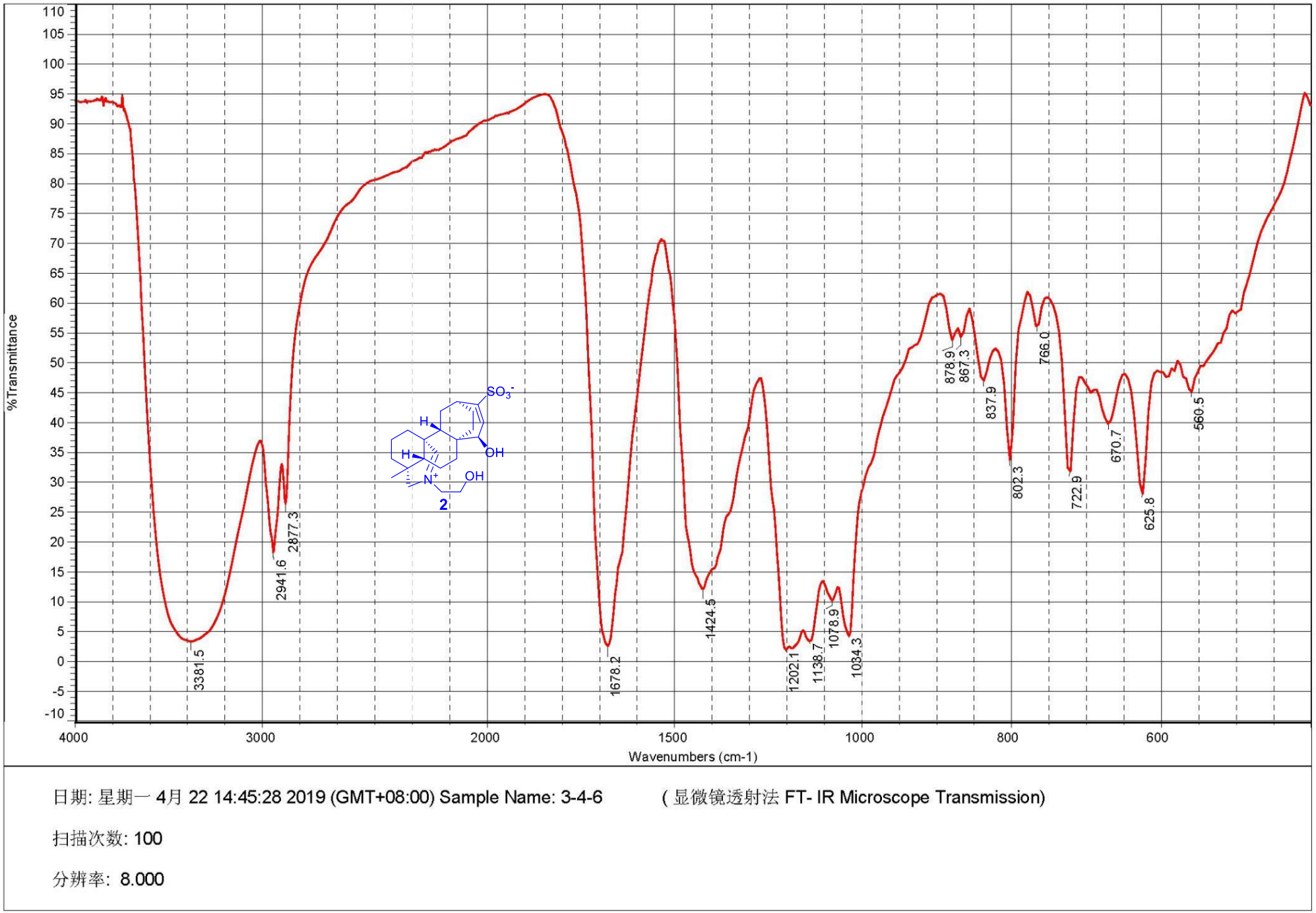

Figure S33. The IR spectrum of **2**.

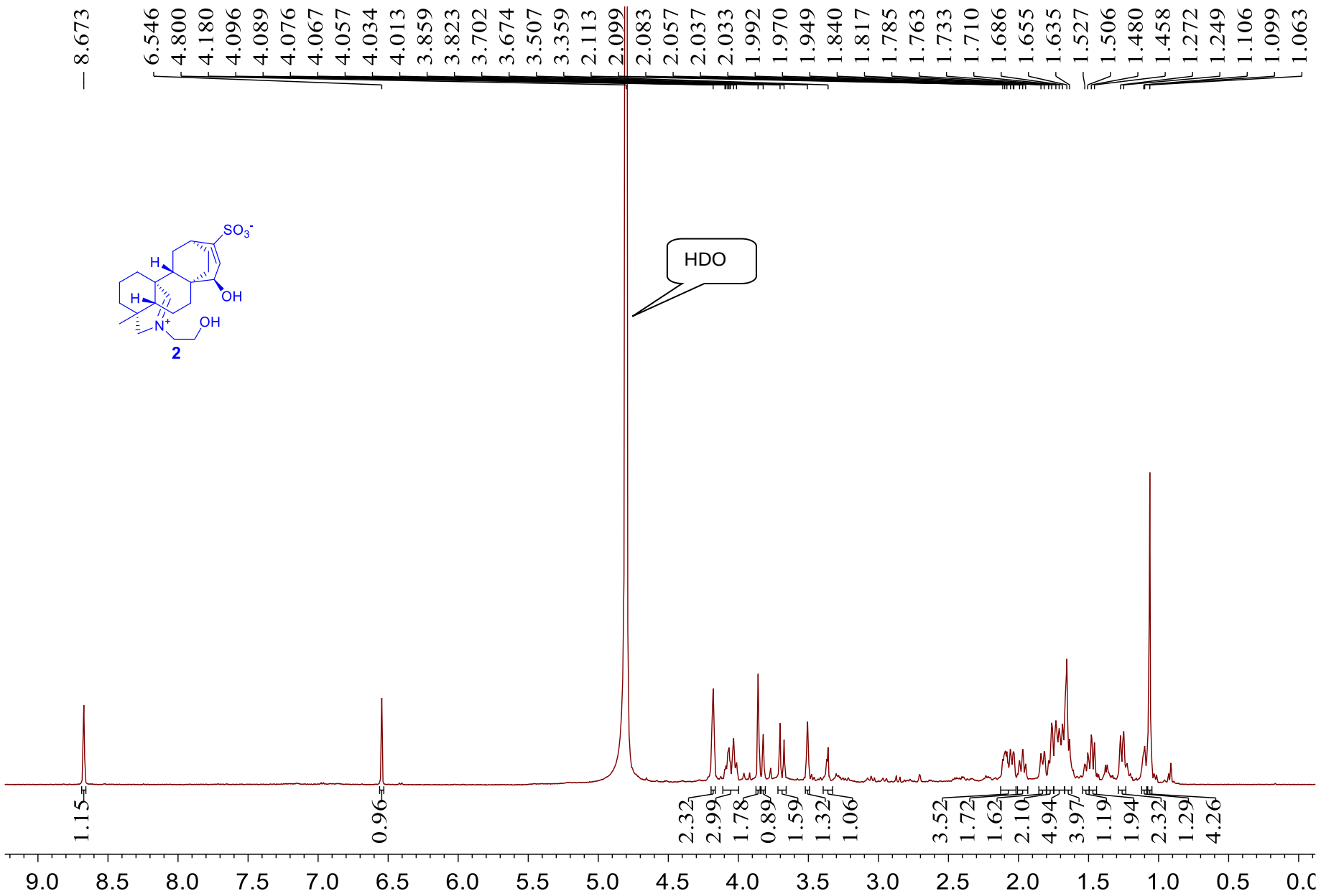

Figure S34. The ^{1}H NMR spectrum of **2** in D_2O (600 MHz).

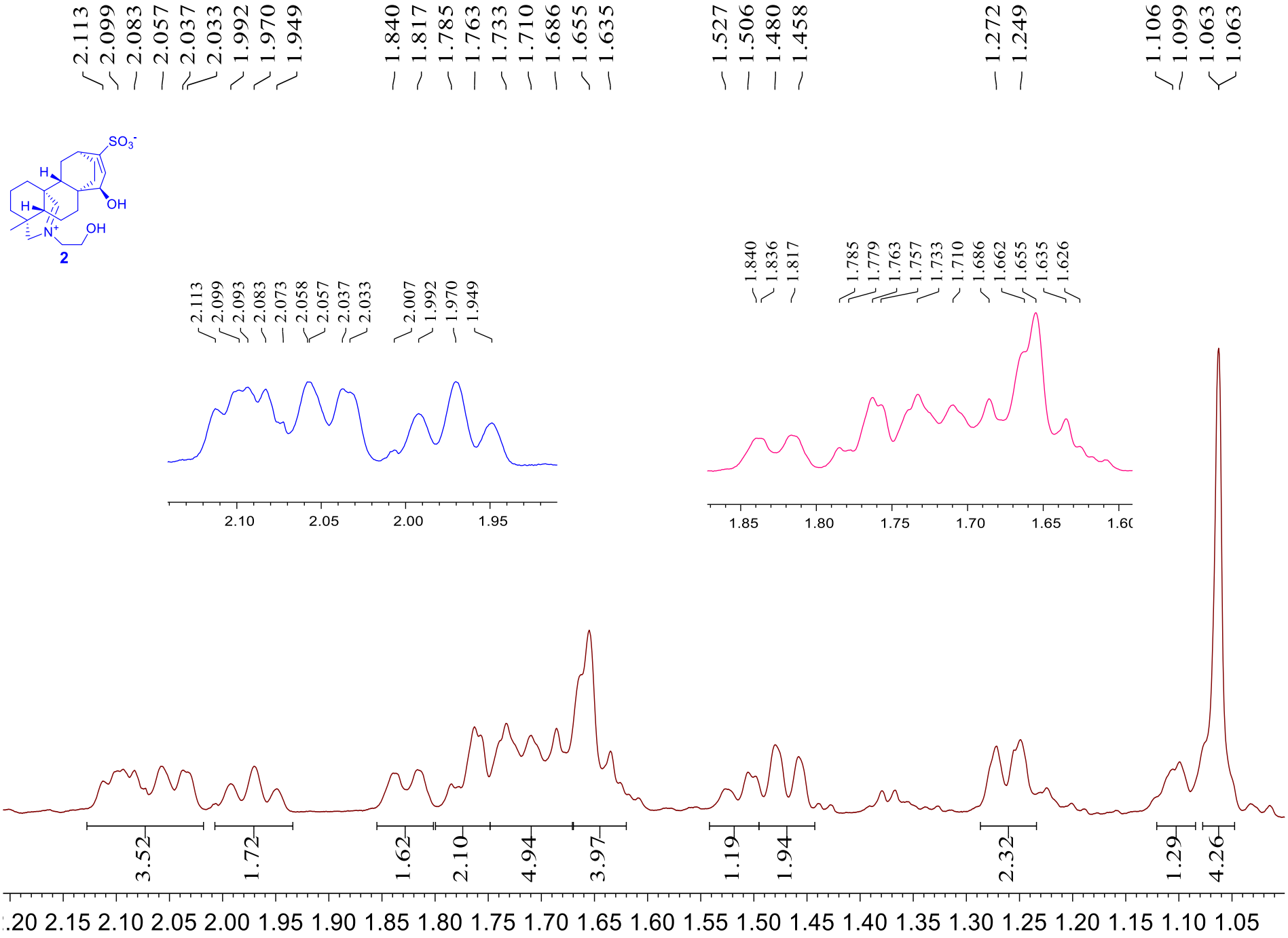

Figure S35. An expansion of 1–2.2 ppm region of the ^{1}H NMR spectrum of **2** in D_2O (600 MHz).

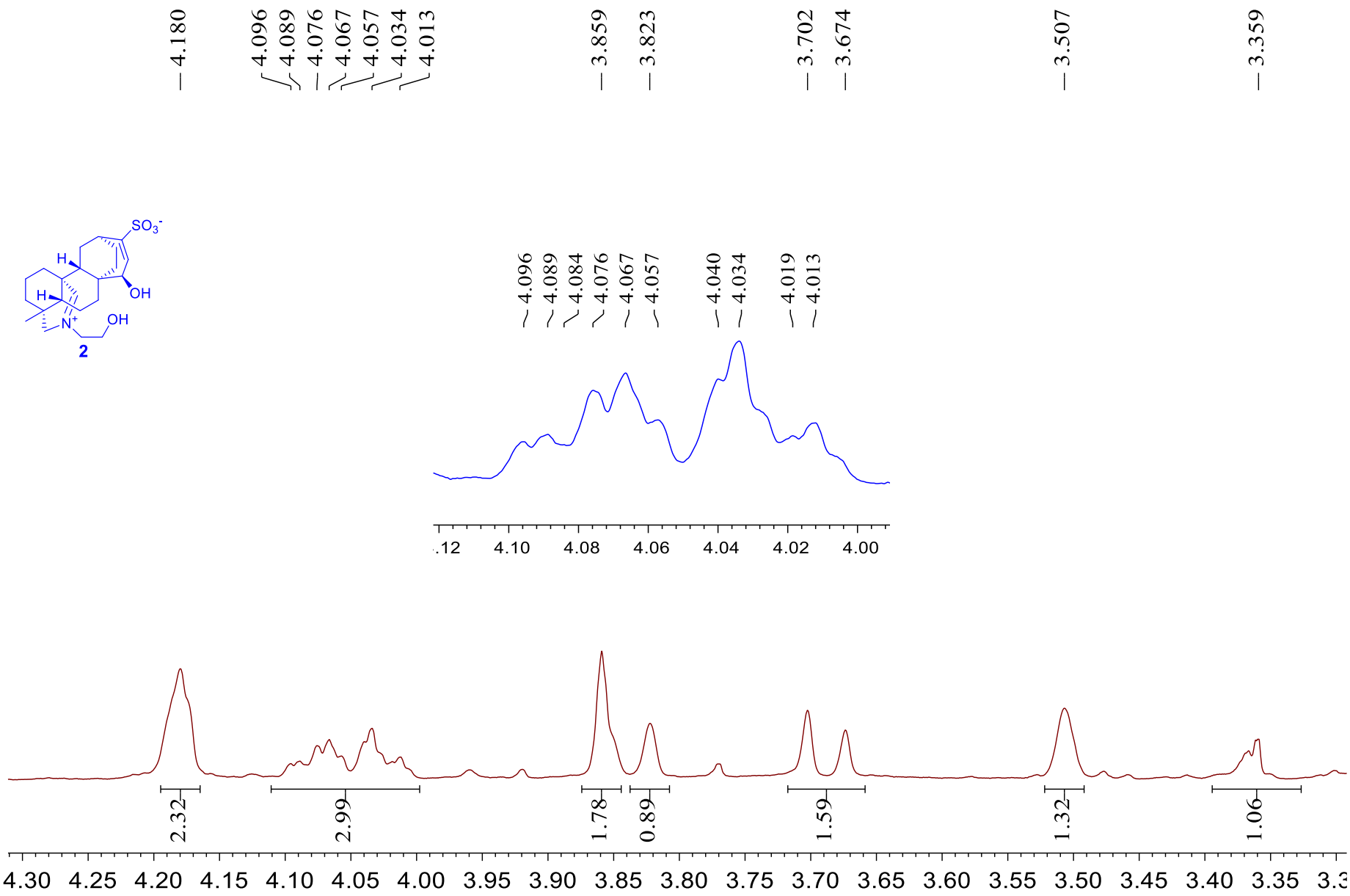

Figure S36. An expansion of 3.3–4.3 ppm region of the ^{1}H NMR spectrum of **2** in D_2O (600 MHz).

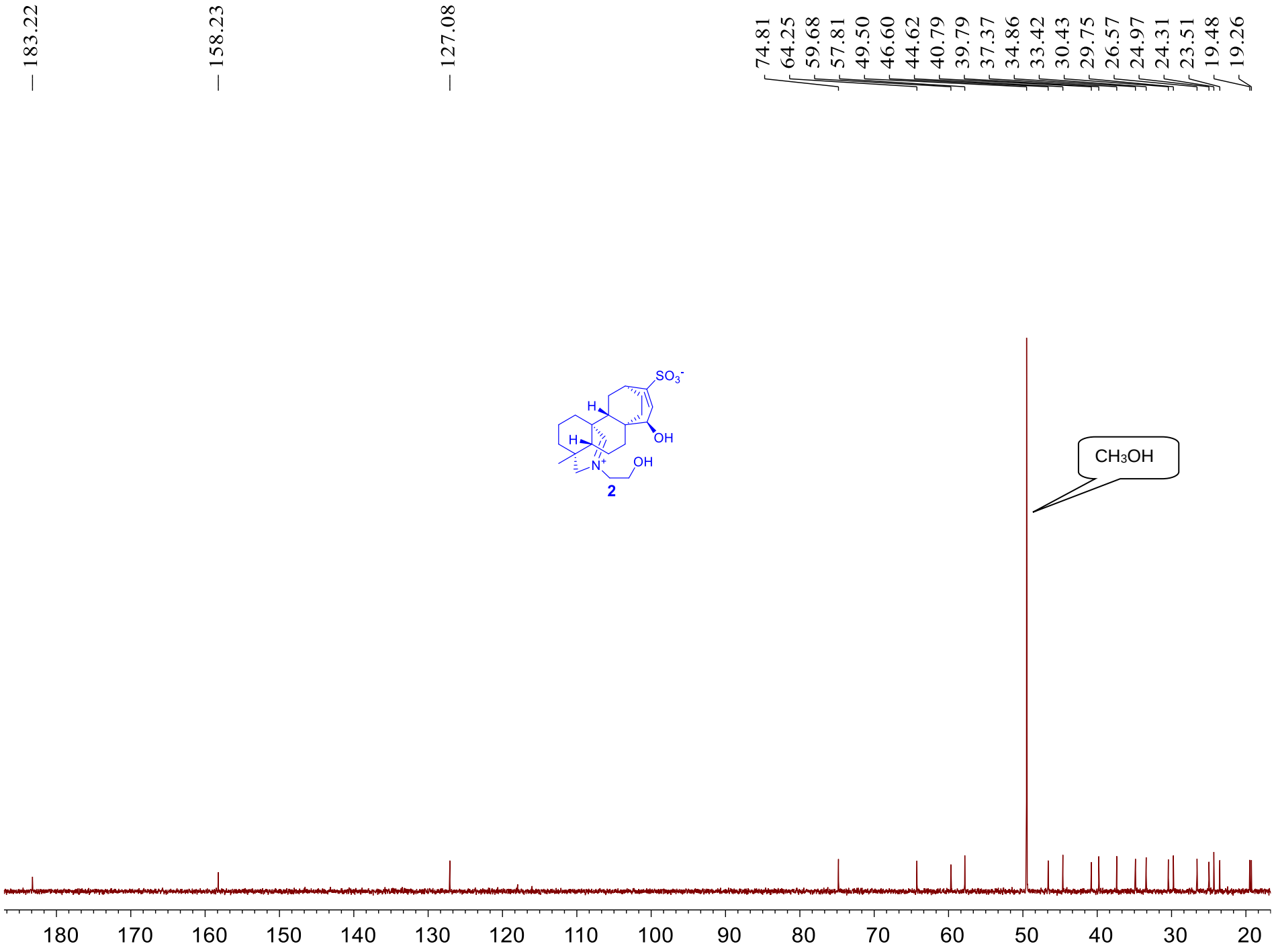

Figure S37. The ^{13}C NMR spectrum of **2** in D_2O (150 MHz).

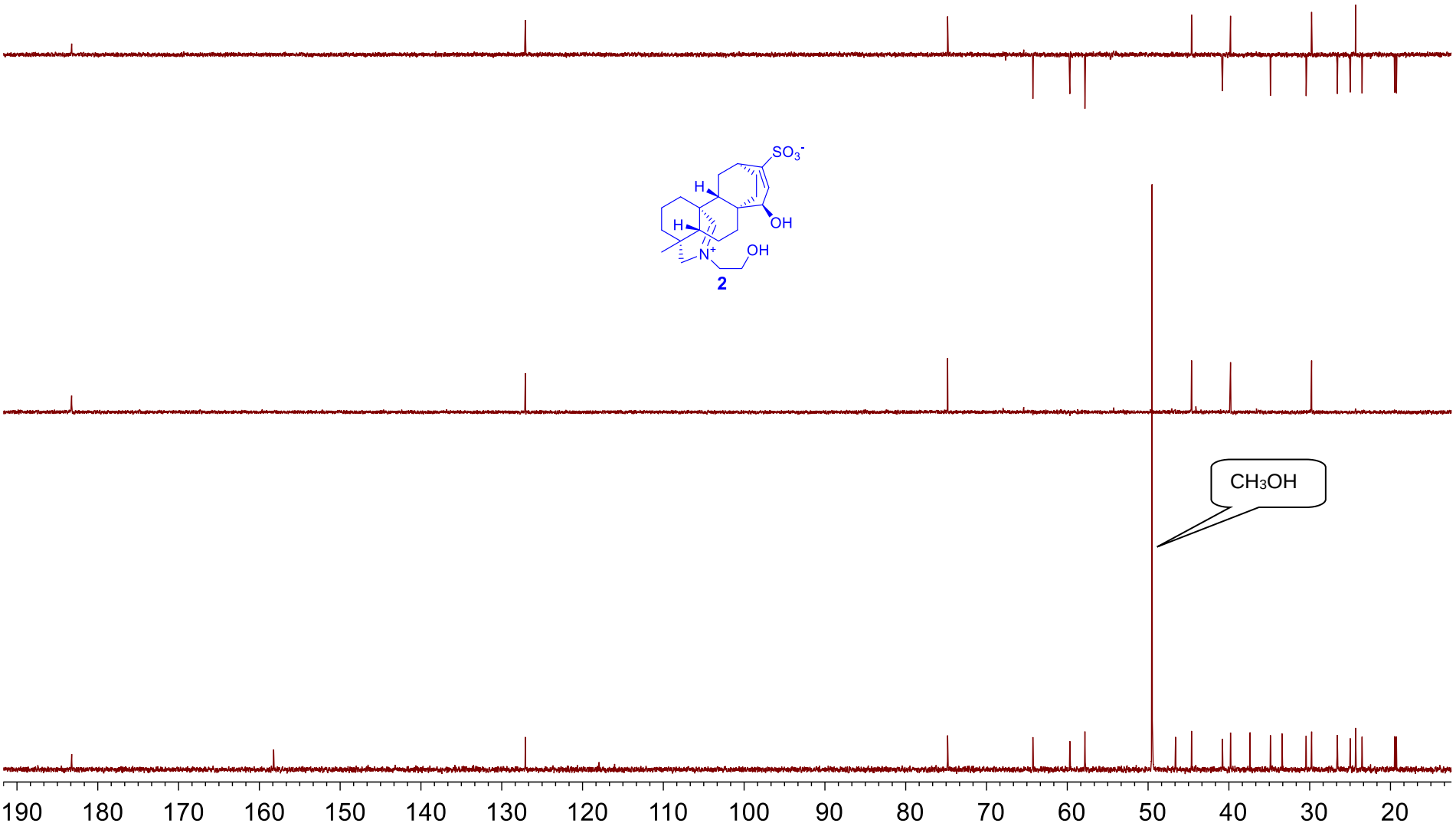

Figure S38. The DEPT spectrum of **2** in D_2O (150 MHz).

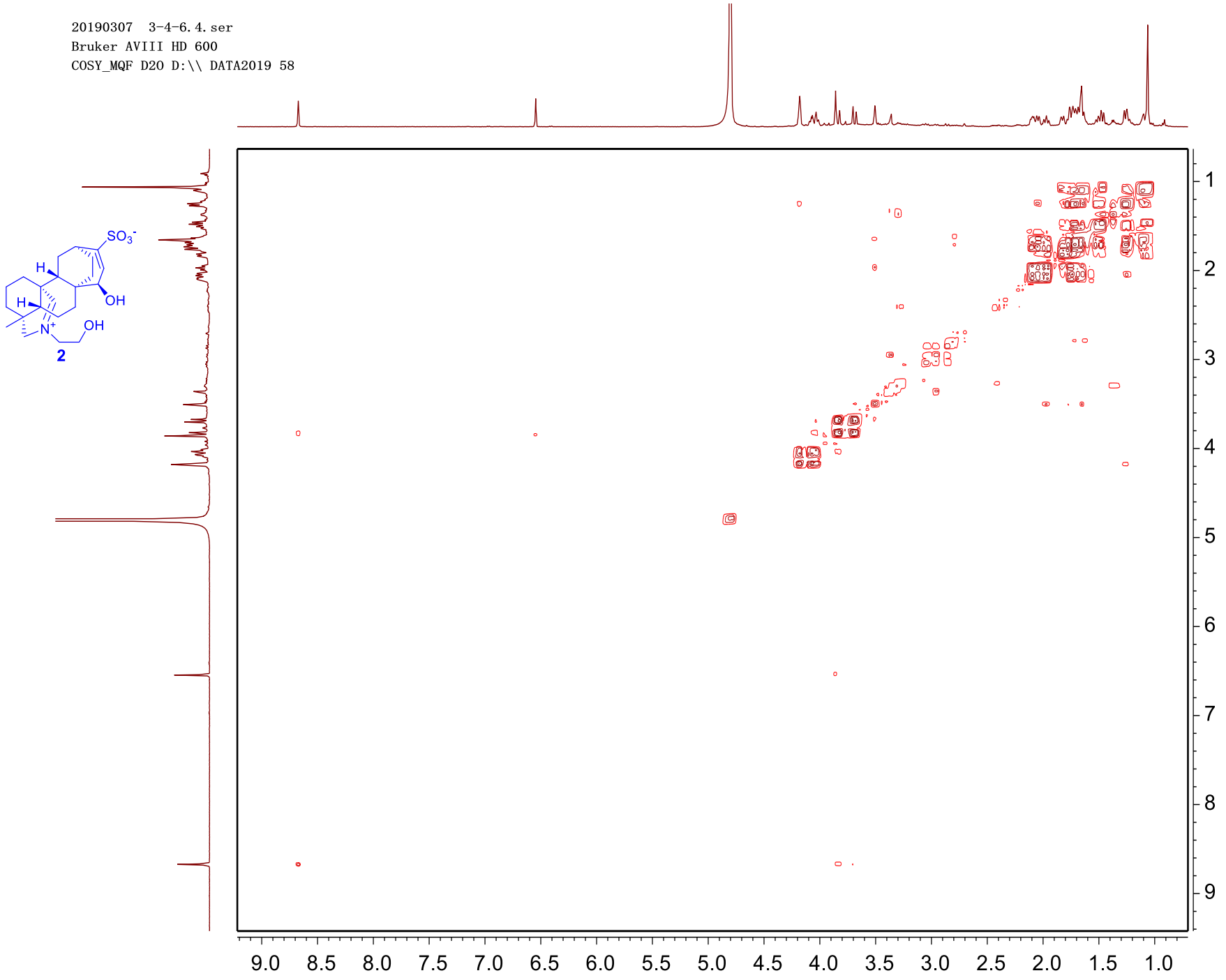

Figure S39. The ^{1}H-^{1}H COSY spectrum of **2** in D_2O (600 MHz).

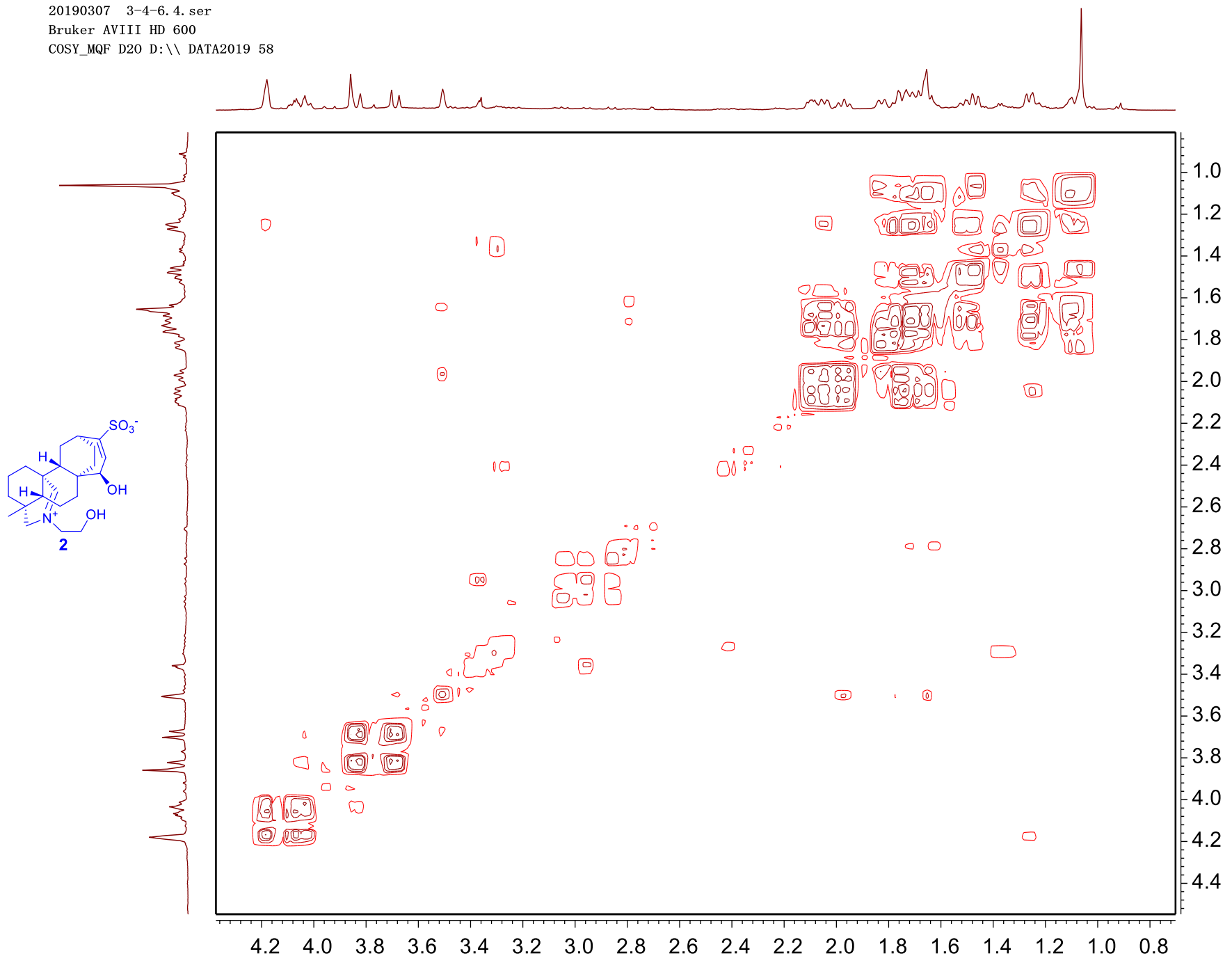

Figure S40. An expansion of 1–4.2 ppm region of the ^{1}H-^{1}H COSY spectrum of **2** in D_2O (600 MHz).

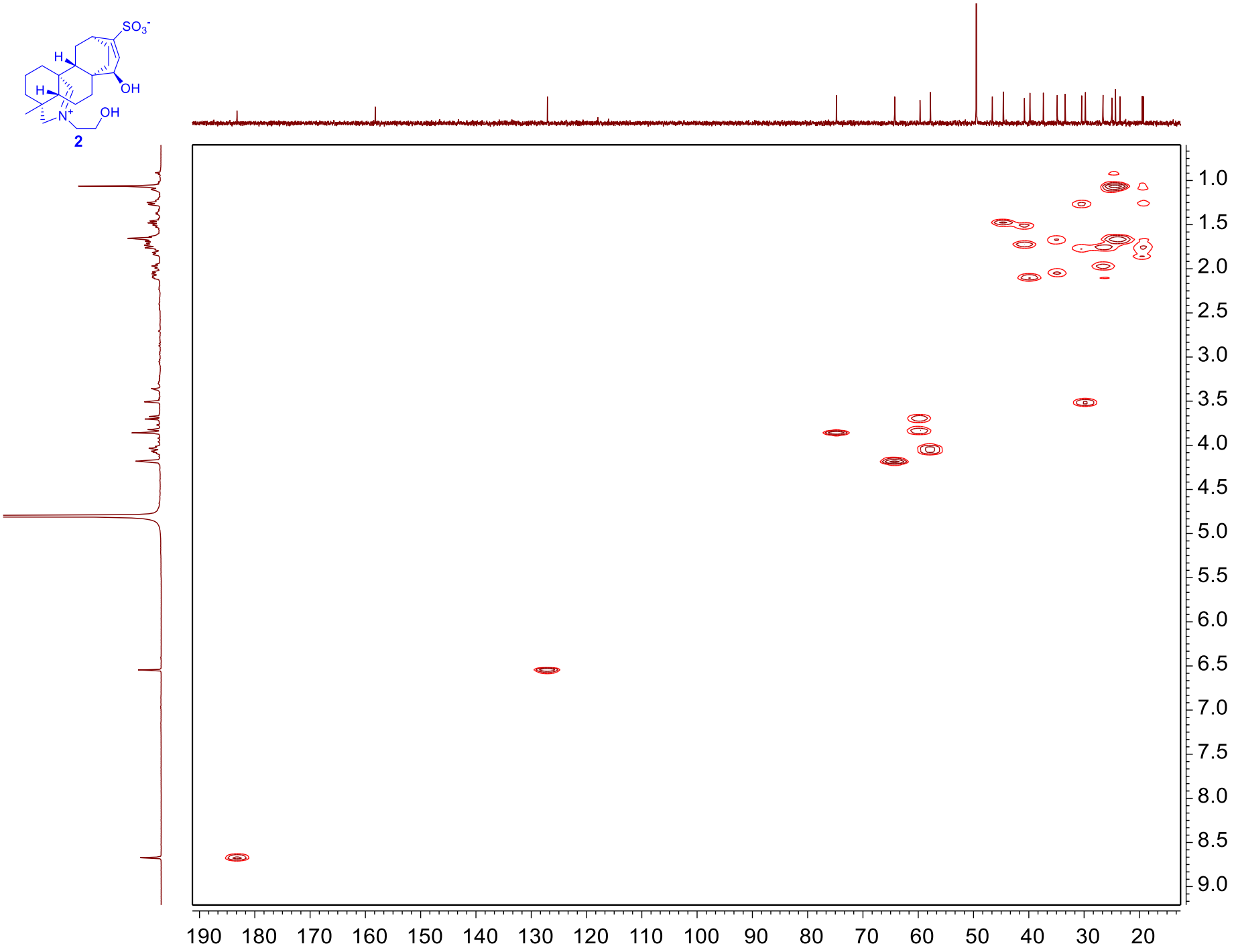

Figure S41. The HSQC spectrum of **2** in D_2O (600 MHz for ^1H).

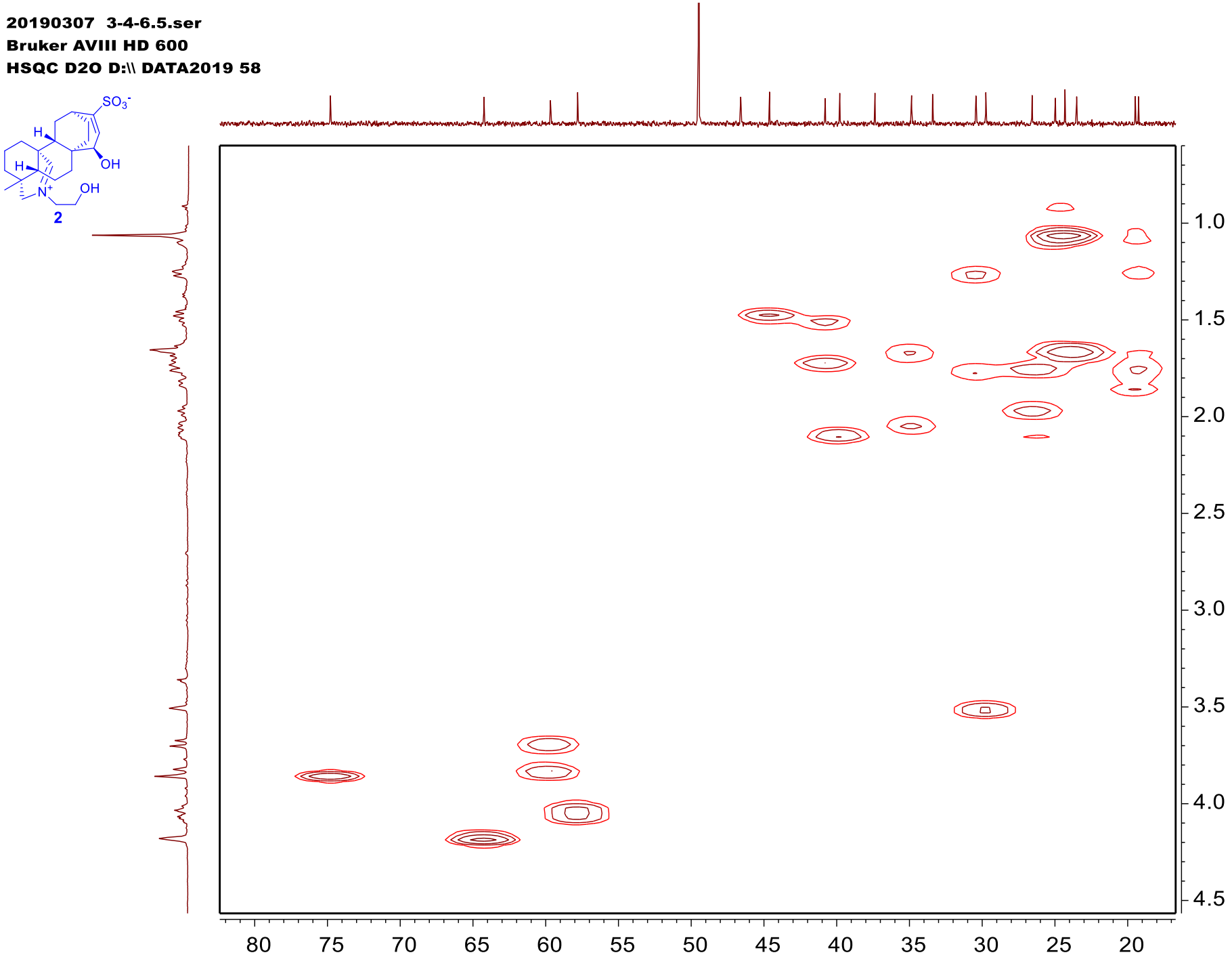

Figure S42. An expansion of 1.0–4.5 (1H)/20–80 (^{13}C) ppm region of the HSQC spectrum of **2** in D_2O (600 MHz for ^{1}H).

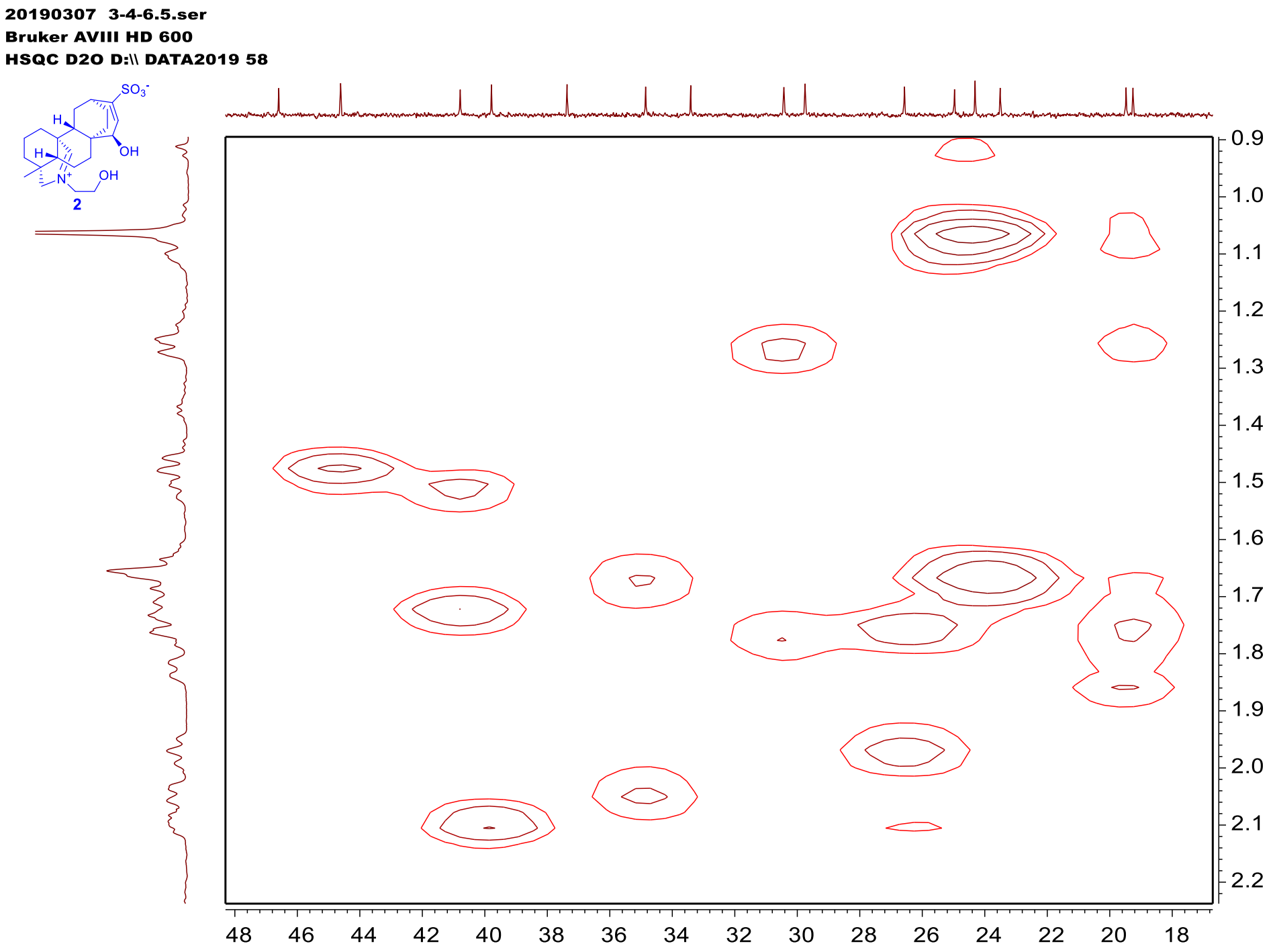

Figure S43. An expansion of 1–2.2 (1H)/20–48 (^{13}C) ppm region of the HSQC spectrum of **2** in D_2O (600 MHz for ^{1}H).

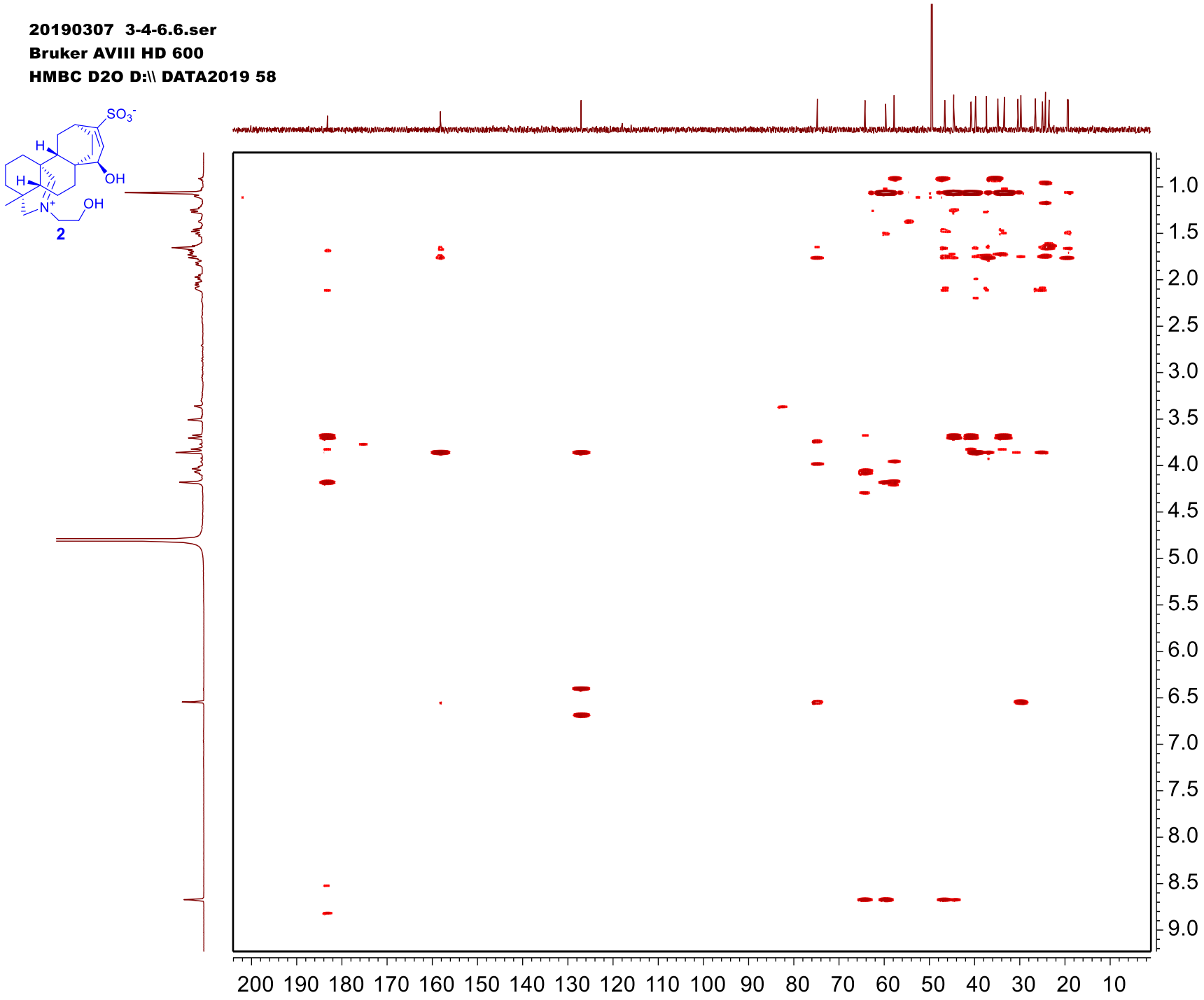

Figure S44. The HMBC spectrum of **2** in D_2O (600 MHz for ^1H).

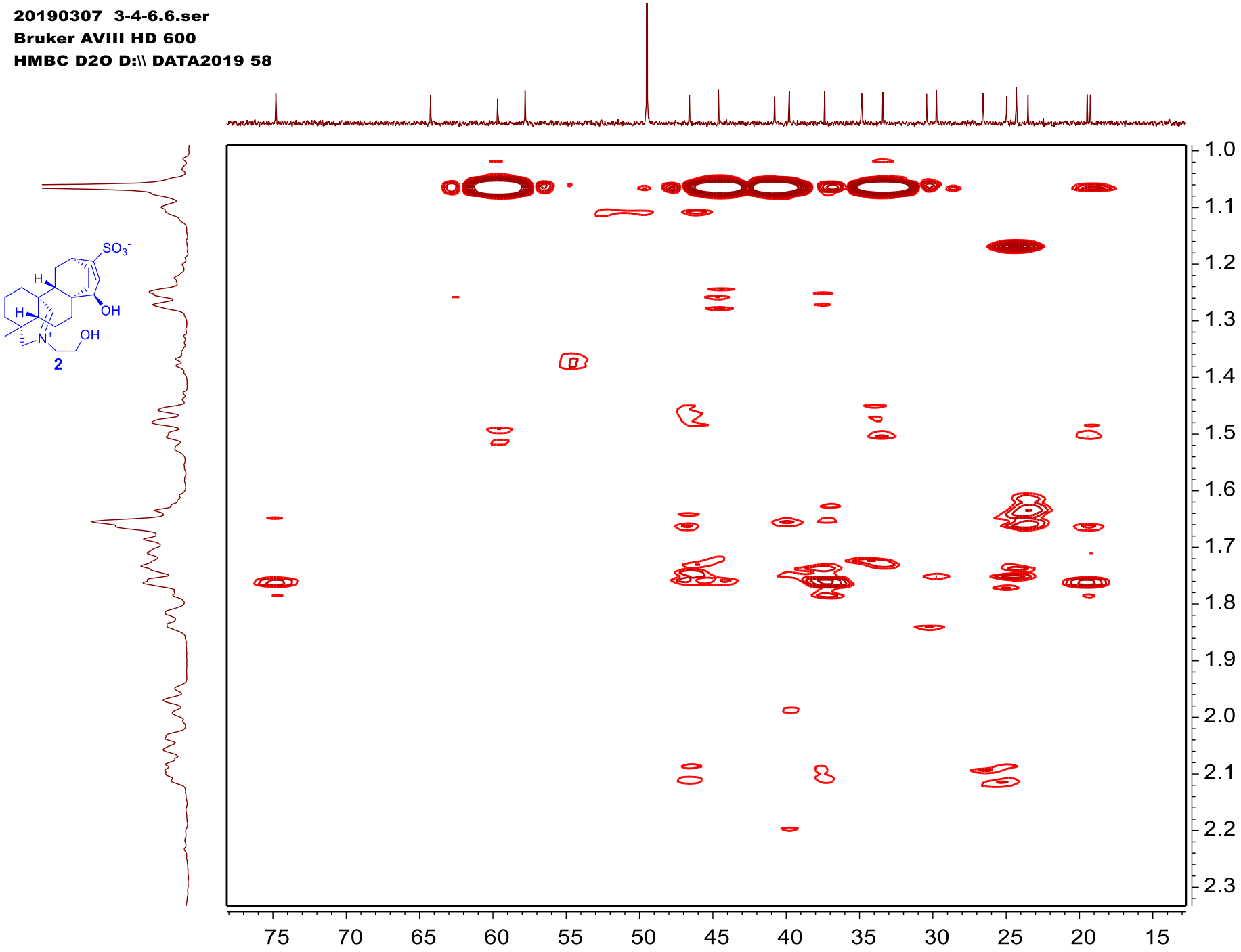

Figure S45. An expansion of the 1–2.3 (^{1}H)/15–75 (^{13}C) ppm region of the HMBC spectrum of compound **2** in D_2O (600 MHz for ^{1}H).

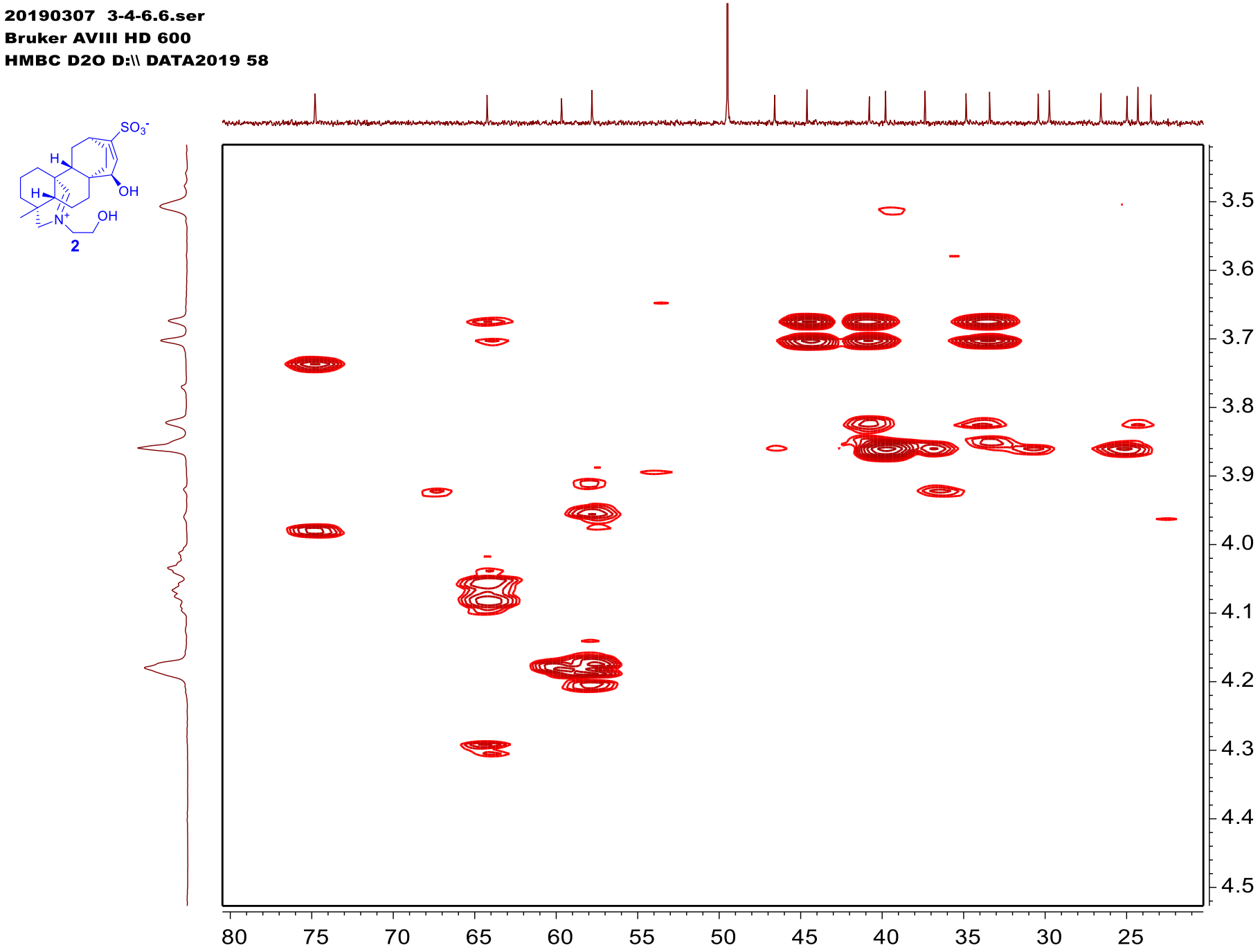

Figure S46. An expansion of 3.5–4.5 (^{1}H)/20–80 (^{13}C) ppm region of the HMBC spectrum of **2** in D_2O (600 MHz for ^{1}H).

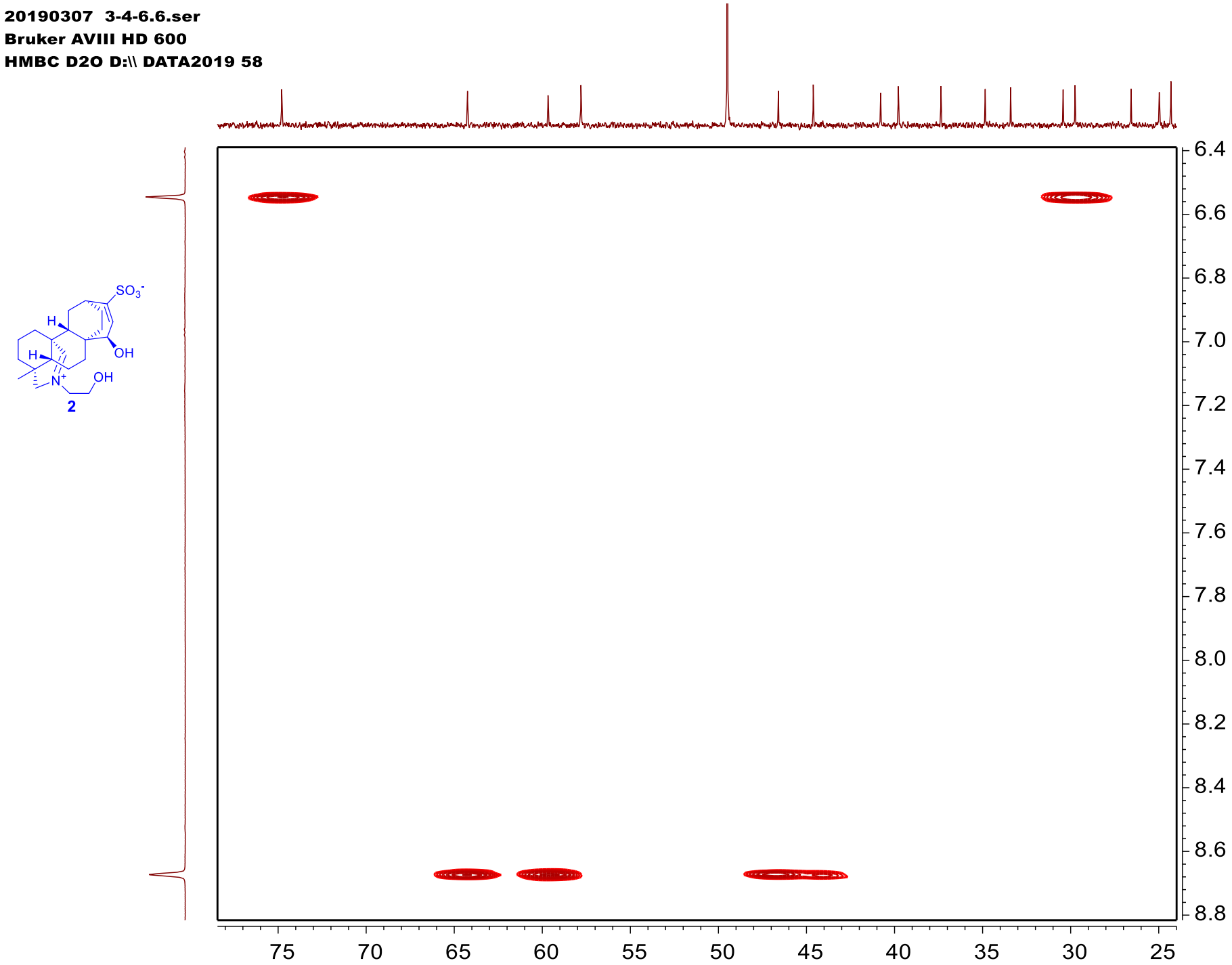

Figure S47. An expansion of 6.4–8.8 (^{1}H)/25–75 (^{13}C) ppm region of the HMBC spectrum of **2** in D_2O (600 MHz for ^{1}H).

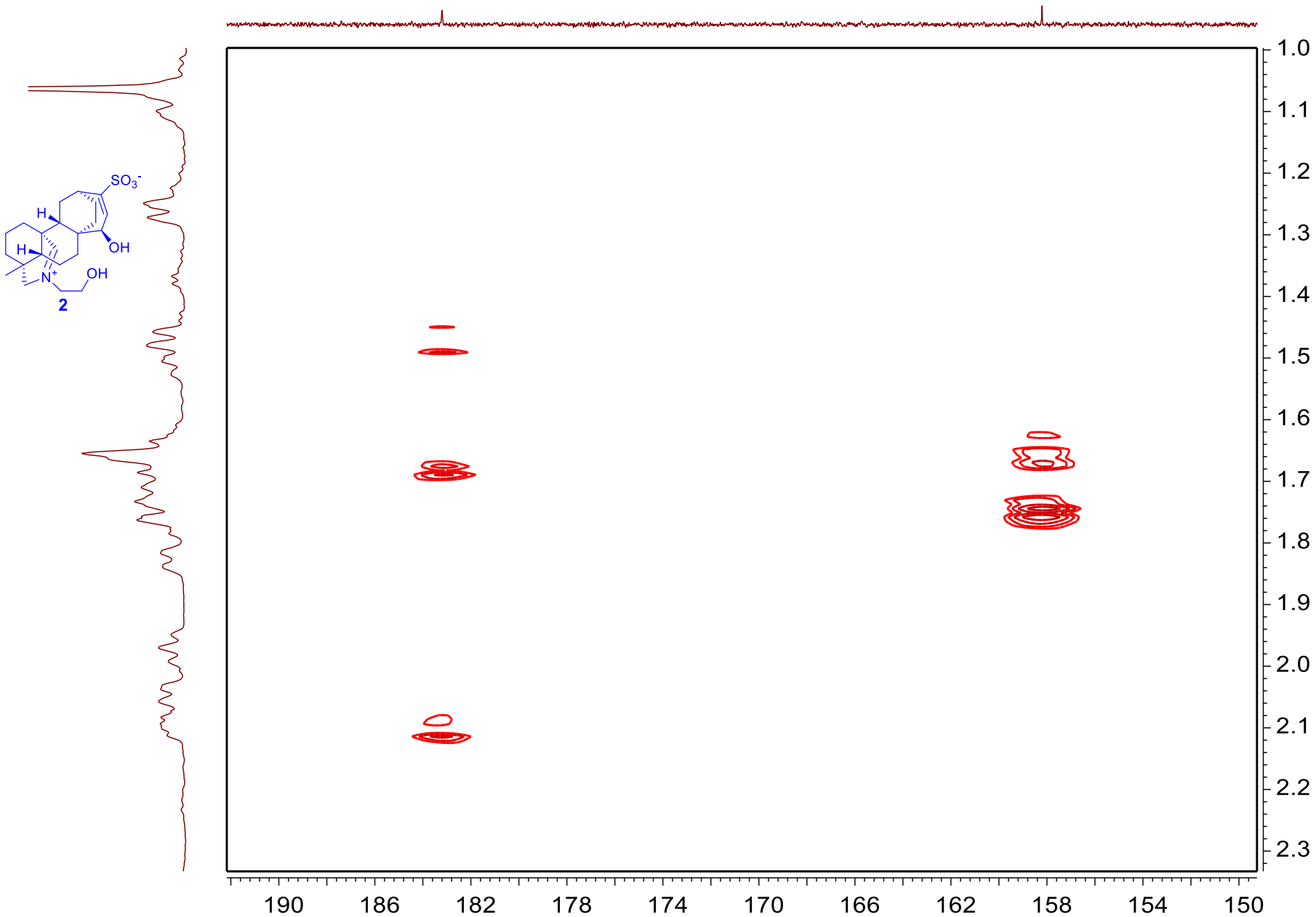

Figure S48. An expansion of 1.0–2.3 (1H)/150–190 (^{13}C) ppm region of the HMBC spectrum of **2** in D_2O (600 MHz for ^{1}H).

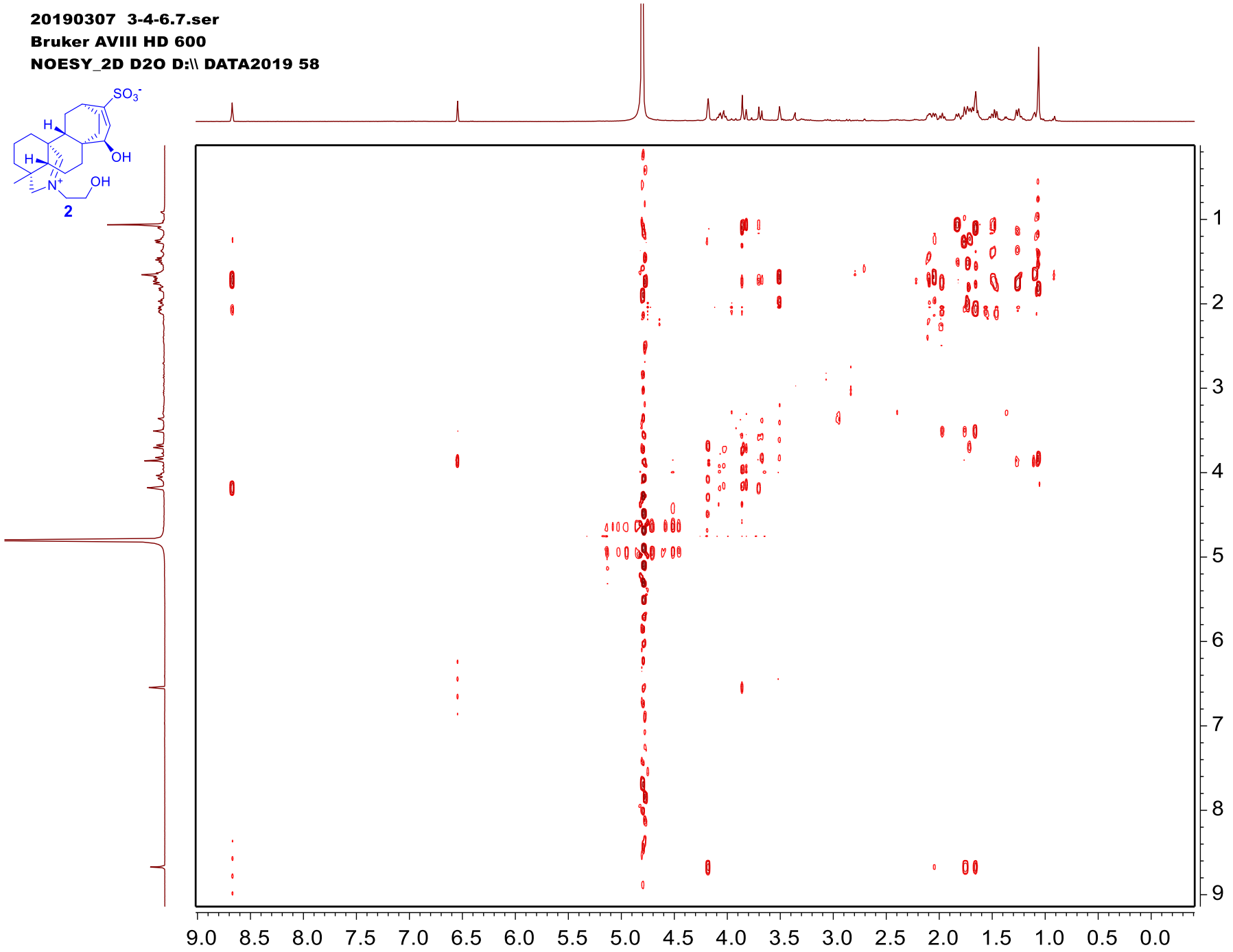

Figure S49. The NOESY spectrum of **2** in D_2O (600 MHz).

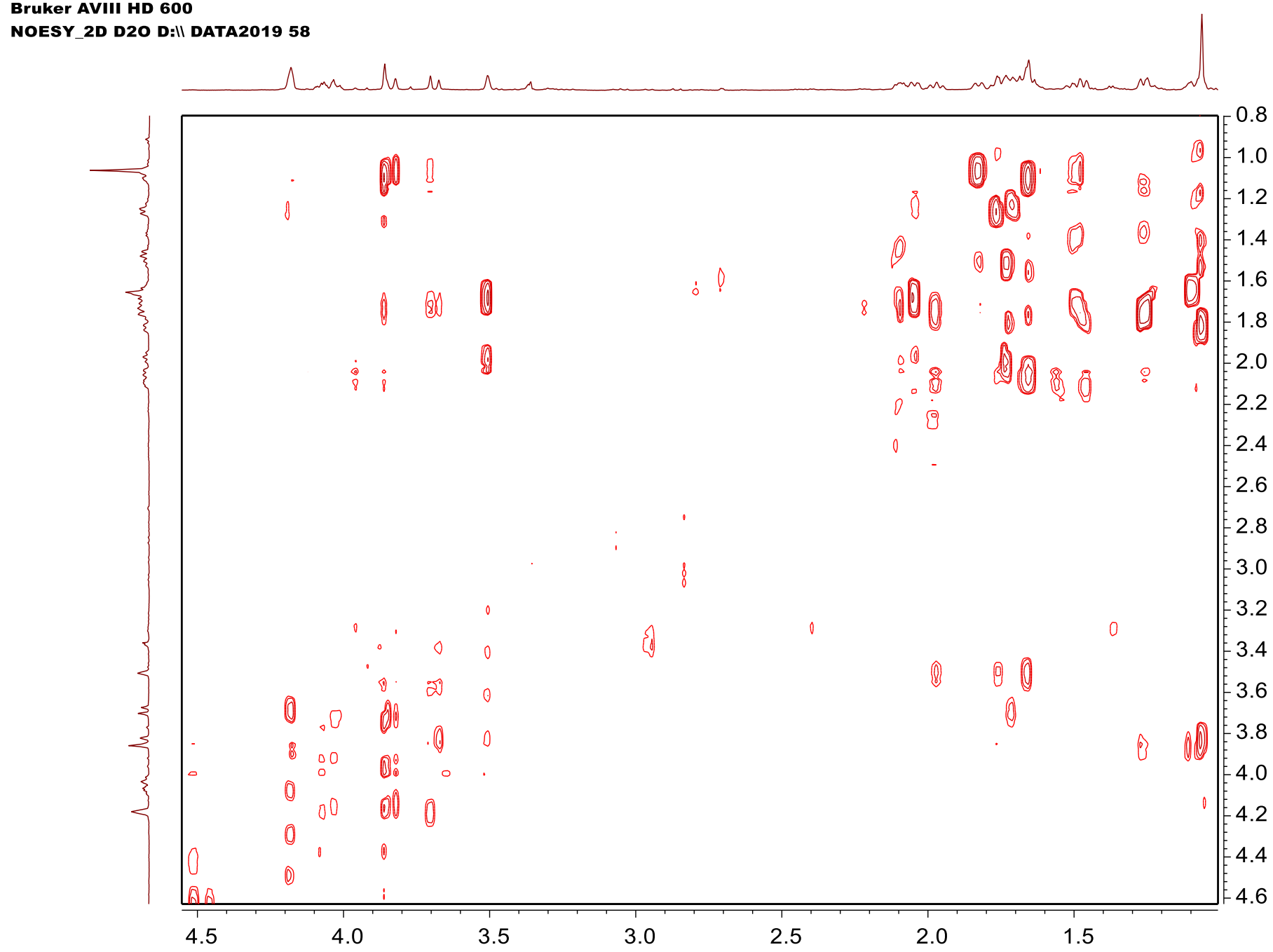

Figure S50. An expansion of 1–4.5 ppm region of the NOESY spectrum of **2** in D_2O (600 MHz).